

Gabriel Barrocas de Oliveira Cruz

**Visualization in micromodels of oil
displacement by O/W emulsions**

Dissertação de Mestrado

Departamento de Engenharia Mecânica

Programa de Pós-Graduação em Engenharia Mecânica

Rio de Janeiro

October 2018



Gabriel Barrocas de Oliveira Cruz

**Visualization in micromodels of oil displacement
by O/W emulsions**

Dissertation presented to the Programa de Pós-Graduação em Engenharia Mecânica of PUC-Rio in partial fulfillment of the requirements for the degree of Mestre em Engenharia Mecânica.

Advisor: Prof. Márcio da Silveira Carvalho

Co-Advisor: Jorge Antonio Avendaño Benavides

Rio de Janeiro

October 2018



Gabriel Barrocas de Oliveira Cruz

**Visualization in micromodels of oil displacement
by O/W emulsions**

Dissertation presented to the Programa de Pós-Graduação em Engenharia Mecânica of PUC-Rio in partial fulfillment of the requirements for the degree of Mestre em Engenharia Mecânica. Approved by the undersigned Examination Committee.

Prof. Márcio da Silveira Carvalho

Advisor

Departamento de Engenharia Mecânica – PUC-Rio

Prof. Paulo Roberto de Souza Mendes

Departamento de Engenharia Mecânica – PUC-Rio

Prof. Abelardo Borges Barreto Junior

Departamento de Engenharia Mecânica – PUC-Rio

Prof. Márcio da Silveira Carvalho

Vice Dean of Graduate Studies

Centro Técnico Científico – PUC-Rio

Rio de Janeiro, October 3rd 2018

All rights reserved.

Gabriel Barrocas de Oliveira Cruz

Bachelor in Engenharia de Petróleo by Pontifícia Universidade Católica do Rio de Janeiro.

Bibliographic data

Cruz, Gabriel Barrocas de Oliveira

Visualization in micromodels of oil displacement by O/W emulsions / Gabriel Barrocas de Oliveira Cruz ; advisor: Márcio da Silveira Carvalho ; co-advisor: Jorge Antonio Avendaño Benavides. – 2018.

99 f. : il. color. ; 30 cm

Dissertação (mestrado)–Pontifícia Universidade Católica do Rio de Janeiro, Departamento de Engenharia Mecânica, 2018.

Inclui bibliografia

1. Engenharia Mecânica – Teses. 2. Microfluídica. 3. Deslocamento imiscível. 4. Injeção de água. 5. Injeção de emulsão. I. Carvalho, Márcio da Silveira. II. Avendaño Benavides, Jorge Antonio. III. Pontifícia Universidade Católica do Rio de Janeiro. Departamento de Engenharia Mecânica. IV. Título.

CDD: 621

To my mother, whose love always guided to me.

Acknowledgments

First, I'd like to thank my parents for always supporting me and believing in me, for the unconditional love that I always received. I am so thankful for all the opportunities you worked so hard for me to have, for teaching me to chase my dreams and that if I fight for something I may achieve it. I love you more than life itself and you are my inspiration, you are what I hope that one day I will be able to be.

I also want to thank my girlfriend Leticia for being the most patient, caring, understanding and awesome person I could ever hope to meet. Thank you for loving me with all my flaws, for calming me when I got desperate and repeating every day that I could, and I would, do it. Thank you for being the reason that I have the strength to fight through anything.

To my friend João thank you for laughing with me of all the crazy things life keep throwing us. For all the coffees, all the talks about books, to making problems seem smaller. For understanding the feeling of making chocolate pudding at 3a.m. because we lost control of our lives.

To professor Márcio for giving me the opportunity to work the laboratory and to make the best project I possibly could. Thank you for being one of the best professors I ever had in my entire life, and to always finding time to help guide me.

To Jorge for being the best co-advisor I could have asked for. Thank you for the patience, for always helping me, even when my questions were stupid, for the constant care and guidance that you gave me through these 2 years. I would never have been able to do any of this without you.

To Felicle and Léo for constantly looking over me in the lab, teaching me everything that I needed to know and having patience every time I did something stupid. Thank you for making the lab a special place to be on.

To Thiago, Marcelo and Mariano for all the laughs and beers shared. Thank you for being awesome buds.

To Maria for, even though she had to leave, keep believing in me and inspiring me to not give up. Thank you for caring so much.

To Julyana and Gisele for being the best IC students anyone could have. I can only hope that I could have been of any assistance to you both.

To Marisa and Nicolle for all the times that you guys talked and helped me in the students room. Both of you are two of the most incredible people I've ever met.

To Mara, Rafael, Rapha, Monique, both Paulos, Paula, Pep, Jose, Lis, Bruna, Débora, Danmer, Fred, Tálita, Pedro, Ranena, to everyone in LMMP all of you helped me so much more than you can ever imagine. Thank you for these two years where I've been so happy to be and to work with all of you.

To PUC-Rio for the scholarship that was given to me, without which this project would not have been possible. Moreover, to Shell for financing the project.

This study was financed in part by the Coordenação de Aperfeiçoamento de Pessoal de Nível Superior – Brasil (CAPES) – Finance Code 001

Abstract

Cruz, Gabriel Barrocas de Oliveira; Carvalho, Márcio da Silveira(Advisor). **Visualization in micromodels of oil displacement by O/W emulsions.** Rio de Janeiro, 2018. 99p. Dissertação de Mestrado – Departamento de Engenharia Mecânica, Pontifícia Universidade Católica do Rio de Janeiro.

The efficiency of water flooding, the most common secondary recovery method in the oil industry, is limited by its non-uniform sweep pattern, originating from the formation of preferential paths because of the high mobility ratio between water and oil, and the high residual oil saturation, associated with capillary oil trapping. In order to improve oil recovery, different approaches have been suggested in the literature, with some of them based on pore blocking and consequent water diversion, thus sweeping a bigger area of the reservoir and displacing more of the trapped oil. Pore blockage can be performed with different methods, one of which is emulsion flooding, with the disperse phase, composed by oil drops, acting as the agent responsible for the decreased water phase mobility. In this work, the fundamental mechanisms of emulsion flooding process was studied experimentally, by visualizing the pore-scale flow in a glass microfluidic device composed of a network of constricted channels, that models the main features of a porous media. The results show the effect of drop size and capillary number on the flow pattern, trapped oil ganglia size and residual oil recovery.

Keywords

Microfluidics; Immiscible Displacement; Waterflooding; Emulsion Flooding.

Resumo

Cruz, Gabriel Barrocas de Oliveira; Carvalho, Márcio da Silveira. **Visualização em micromodelos da recuperação de óleo por emulsões O/W**. Rio de Janeiro, 2018. 99p. Dissertação de Mestrado – Departamento de Engenharia Mecânica, Pontifícia Universidade Católica do Rio de Janeiro

A eficiência do processo de injeção de água, o método de recuperação secundária mais comum na indústria do petróleo, é limitada por seu padrão de varredura não uniforme, originado da formação de caminhos preferenciais devido à alta razão de mobilidade entre água e óleo, e a elevada saturação de óleo residual, associada aos efeitos capilares. A fim de melhorar a recuperação de petróleo, diferentes abordagens têm sido sugeridas na literatura, com algumas delas baseadas no bloqueio de poros e consequente desvio de água, varrendo assim uma área maior do reservatório e deslocando mais do óleo aprisionado por capilaridade. O bloqueio de poros pode ser realizado com diferentes métodos, sendo um deles a injeção de emulsão, com a fase dispersa, composta por gotas de óleo, atuando como o agente responsável pela diminuição da mobilidade da fase aquosa. Neste trabalho, os mecanismos fundamentais do processo de injeção de emulsão foram estudados experimentalmente, visualizando-se o escoamento em escala de poros em um dispositivo micro-fluídico de vidro composto por uma rede de canais constritos, que modela as principais características de um meio poroso. Os resultados mostram o efeito do tamanho da gota e do número de capilaridade no padrão do escoamento, no tamanho dos gânglios do óleo aprisionado e na recuperação de óleo residual.

Palavras chave

Microfluídica; Deslocamento Imiscível; Injeção de Água; Injeção de Emulsão

Table of contents

| | | |
|-------|--|----|
| 1 | Introduction | 15 |
| 1.1 | Motivation | 15 |
| 1.2 | Fundamental Concepts | 15 |
| 1.2.1 | Flow in Porous Media | 15 |
| 1.2.2 | Two-Phase Flow in Porous Media..... | 17 |
| 1.2.3 | Flooding as an EOR Method | 22 |
| 1.3 | State of Art | 34 |
| 1.4 | Objectives | 37 |
| 2 | Experimental Approach..... | 38 |
| 2.1 | Material and Methods..... | 38 |
| 2.1.1 | Micromodels..... | 39 |
| 2.1.2 | Injection System | 45 |
| 2.1.3 | Solutions | 47 |
| 2.1.4 | Image Acquisition and Analysis System..... | 49 |
| 2.1.5 | Emulsions | 51 |
| 2.2 | Experimental Setup | 53 |
| 2.2.1 | Emulsion Production | 53 |
| 2.2.2 | Fluid Injection in Porous Media | 55 |
| 2.3 | Experimental Procedure | 57 |
| 3 | Results and Discussions | 62 |
| 3.1 | Emulsion Production | 63 |
| 3.2 | Low Capillary Number..... | 64 |
| 3.2.1 | Residual Oil Saturation..... | 65 |

| | |
|-------------------------------------|----|
| 3.2.2 Emulsions Size Analysis | 66 |
| 3.3 Higher Capillary Number | 86 |
| 3.3.1 Residual Oil Saturation..... | 87 |
| 3.3.2 Drops Sizes | 89 |
| 4 Conclusion..... | 95 |
| Bibliography | 97 |

List of Figures

| | |
|---|----|
| Figure 1- Contact angle between water and surfaces with different wettability. | 19 |
| Figure 2- Relative permeability curves on the left with the drainage process and in the right the imbibition process. | 20 |
| Figure 3- Residual oil saturation variation with the injecting capillary number for different permeability | 22 |
| Figure 4- Viscous fingering in a water flooding..... | 24 |
| Figure 5- Illustration of pore blockage during emulsion flooding, altering the preferential paths of the water. | 25 |
| Figure 6- Two phase emulsions..... | 26 |
| Figure 7- Surfactant in emulsions. | 27 |
| Figure 8- Surface Tension variation with surfactant concentration, and illustration of micelle formation on the CMC. | 28 |
| Figure 9- Schematic representation of instability process in emulsions. | 30 |
| Figure 10- Emulsions being formed through squeezing, the dispersed phase presented as orange and the continuous phase as blue | 32 |
| Figure 11- Emulsions being formed through jetting, the dispersed phase presented as orange and the continuous phase as blue | 33 |
| Figure 12- Emulsions being formed through dripping, the dispersed phase presented as orange and the continuous phase as blue | 33 |
| Figure 13- Connector utilized in the devices..... | 40 |
| Figure 14- Droplet Junction Chip made by Dolomite | 41 |
| Figure 15 – Schemed image of the microfluidics device used for the emulsion formation, with focus in the T-Section. | 42 |
| Figure 16- Porous media device. | 42 |
| Figure 17- Schematic view of the porous media device..... | 43 |
| Figure 18- Randomized pattern of channels and throats repeated in the porous media. | 44 |
| Figure 19- Model of the utilized syringe pumps during the experiments | 46 |
| Figure 20- Microscope used for image acquisition. | 49 |

| | |
|--|----|
| Figure 21- Process of emulsion creation, with the large on the left and the small on the right..... | 51 |
| Figure 22 Emulsion droplets, largest and smallest size..... | 52 |
| Figure 23- Experimental set-up used for the production of emulsion..... | 54 |
| Figure 24- Schematic view of the experimental setup | 55 |
| Figure 25- Experimental set-up utilized during the emulsion flooding | 56 |
| Figure 26- Regions of the micromodel..... | 57 |
| Figure 27- Software utilized for the acquisition of the images in the microscope after the experiment..... | 58 |
| Figure 28-Sections A13 and A14 of the micromodel after the emulsion flooding of the 175 μ m drops. Aqueous phase colored with a red dye, droplets colored with a black dye and oil transparent..... | 59 |
| Figure 29- Sections A13 and A14 after a water flooding after and before the macro. Up before the macro with the water as red and the oil as transparent, beneath after the macro with the water white and the oil black..... | 60 |
| Figure 30 Images of the micromodel after the water flooding and emulsion flooding of the experiments performed at a $Ca=3.5 \times 10^{-7}$ and with dispersed phase of the emulsions with a size of 175 μ m. Flow from top to bottom | 68 |
| Figure 31- Section of the porous media after emulsion flooding with large drops exemplifying their deformation..... | 70 |
| Figure 32- Drop distribution along the porous media in experiment performed with droplets of 175 μ m | 71 |
| Figure 33- Difference in the drops in the entrance and the exit of the porous media, left and right respectively. | 73 |
| Figure 34- Images of the micromodel after the water flooding and emulsion flooding of the experiments performed at a $Ca=3.5 \times 10^{-7}$ and with dispersed phase of the emulsions with a size of 120 μ m. Flow from top to bottom | 74 |
| Figure 35- Drop distribution along the porous media in experiment performed with droplets of 120 μ m | 76 |
| Figure 36- Droplet size distribution along the micromodel for injection of drops of 120 μ m with a $Ca = 3.5 \times 10^{-7}$ | 77 |

| | |
|---|----|
| Figure 37- Drop Size distribution of the porous media at 0.065ml/h and a dispersed phase of 120µm. | 78 |
| Figure 38: Images of the micromodel after the water flooding and emulsion flooding of the experiments performed at a $Ca=3.5 \times 10^{-7}$ and with dispersed phase of the emulsions with a size of 80µm. Flow from top to bottom. | 80 |
| Figure 39- Pore blockage by an agglomeration of the smaller sized emulsions above comparing to the blockage by a single droplet in the flooding with the larger size below. | 82 |
| Figure 40- Drop distribution along the porous media in experiment performed with droplets of 80µm. | 83 |
| Figure 41- Droplet size distribution along the micromodel for injection of drops of 80µm with a $Ca = 3.5 \times 10^{-7}$ | 84 |
| Figure 42- Drop Size distribution in the porous media at 0.065ml/h and a dispersed phase of 80µm. | 85 |
| Figure 43: Images of the micromodel after the water flooding and emulsion flooding of the experiments performed at a $Ca=1.85 \times 10^{-6}$ and with dispersed phase of the emulsions with a size of 175µm. | 89 |
| Figure 44: Images of the micromodel after the water flooding and emulsion flooding of the experiments performed at a $Ca=1.85 \times 10^{-6}$ and with dispersed phase of the emulsions with a size of 120µm. | 90 |
| Figure 45: Images of the micromodel after the water flooding and emulsion flooding of the experiments performed at a $Ca=1.85 \times 10^{-6}$ and with dispersed phase of the emulsions with a size of 80µm. | 91 |
| Figure 46- Drop distribution along the porous media in experiment performed with droplets of 175µm | 93 |
| Figure 47- Drop distribution along the porous media in experiment performed with droplets of 120µm | 93 |
| Figure 48- Drop distribution along the porous media in experiment performed with droplets of 80µm | 94 |

1

Introduction

1.1

Motivation

The total worldwide energy requirement has been growing in recent years leading to an increase necessity in hydrocarbon production. This increase in demand led to the development of enhanced recovery methods for oil fields, as the processes traditionally used leave a considerable amount of the original oil in place in the reservoir at the end of the operation.

An oil field has an internal energy through which the early steps of the oil recovery is carried out, called the primary recovery. When the internal energy of the reservoir starts to decline during the production, and the rate of oil recovery suffers a reduction as well, it becomes necessary to infuse the reservoir with energy coming from outside, usually done with the injection of a fluid in the reservoir; this process is usually known as secondary recovery.

Water flooding is the most common method of secondary recovery used in the industry, but the recovery attained from this process is limited, due to the usual early arrival of the injected water in the producing well, which happens because of the high mobility of the water in comparison to the oil. As a result, preferential paths of water appears and leads to a low sweep efficiency in the water flooding process. The sweep efficiency is a parameter used to analyze a recovery process and it is evaluated as the ratio between the invaded volume by the injected fluid and the total volume of the reservoir.

Different technologies and methodologies have been tried to improve water flooding recovery, one of such involves the injection of emulsion in the reservoir. In the oil industry, emulsion study is important as they may be responsible for problems that may occur during production but may be beneficial when intentionally injected in the reservoir under specific conditions. The use of emulsion flooding between two water flooding, process called water alternate emulsion (WAE), has been shown to result in an improvement in the recovery factor due, among other factors, the water phase mobility reduction generated with the emulsion injection through the blockage of pores in the preferential paths, leading to a reduction of the effective permeability of these zones.

Emulsion flooding is a complex process and although experimental evidences have proven its positive effects, the pore scale mechanisms and the effect of different process variables in flow diversion is still not fully understood. Due to this, it is important to extend new studies on the process for a better understanding on the most influential aspects and optimize it to use the emulsion injection as a mobility control process. Visualization of the behavior of the emulsion displacement at microscale is an important study for this purpose, with specially attention to the pore blocking mechanism and the resulting flow diversion.

1.2

Fundamental Concepts

1.2.1

Flow in Porous Media

Fluid flow in porous media is an important area of analysis in many fields of studies and in different areas of technology, resulting in a plethora of aspects. For this work, the focus will be from the oil industry point of view, where is of vital importance as the oil reservoir is a porous media itself, usually composed of sedimentary rocks,

where most secondary and enhanced recovery methods success depend on the good understanding of the flow conditions.

Fluid flow in a porous media is based on Darcy's Law, which describes the relation between the flow rate and the pressure gradient. In a simplified form, it is described as:

$$\frac{q}{A} = - \frac{k}{\mu_f} \frac{\Delta P}{L} = v \quad (1)$$

In this equation k represent the permeability of the porous media, μ_f is the viscosity of the working fluid and ρ_f is its density. ΔP is the pressure drop that the fluid is submitted to. v is the Darcy velocity of the fluid, which is the flow rate (q) divided by the cross-sectional area (A) through which the flow is occurring.

This law indicates one important aspect for the comprehension and analysis of the flow, there is a linear correlation between the flow rate of the fluid and the pressure gradient in porous media. The negative sign indicates the direction of the flow, with it occurring from the area of higher pressure to the area of lower pressure. This aspect of the flow is the main reason why, during oil production after long stretches of time, the oil recovery rate starts to decline. As the fluids are produced, their saturation in the reservoir starts to decline leading to a reduction in the internal pressure of the system and subsequently to the volume of oil recovered. [1].

It is important to understand that although one of the equations that govern the flow through porous media, Darcy's Law have some limitations in its usage. For an accurate result it requires a steady-state regime, there is a necessity of the porous media to already be saturated with the fluid of interest and in low permeability porous media studies have shown that the characteristics of the flow demonstrates discrepancies when compared to Darcy's law [2].

Porosity is a another aspect of a porous media that directly affects the flow, it is defined as a relation between the volume of voids in a material compared to its total

volume. The porosity of a medium only represents the presence of void spaces not indicating how accessible those spaces are though, so it may not strictly represent how easily a fluid is able to flow through it, for a better evaluation of this aspect the permeability is the most representative property of a porous media.

The permeability of a porous media, is a property that measures the capacity of a fluid to pass through its pores or fractures. The permeability is a characteristic of the geometry of the mediums grains and pores, with a tendency to decrease with smaller grain sizes and being negatively affected by a matrix composed of distinct grains sizes, and has a direct correlation to how well connected the pores are [3].

When analyzing the permeability in a porous media there are a few important aspects that should be taken under consideration such as the homogeneity of the medium, as a global permeability value may be masking different zones with distinct permeability values, affecting the flow. In an anisotropic porous media, the local permeability indicates the direction that a passing fluid will most likely flow through, indicating the directional movement in the porous media.

1.2.2

Two-Phase Flow in Porous Media

In oil reservoirs, a porous media hardly ever is completely saturated with a single fluid, usually with flows occurring with the presence of two immiscible fluids, such as oil and water. In such scenarios, one fluid directly affects the others due to its characteristics and interactions with each other and with the medium, as well as with their flow. With the presence of one fluid affecting the others, it is not possible to study only the fluid of interest acting as a single-phase flow while ignoring the others, instead having to study the system as a whole and the effects and forces in display. That said, it is necessary to define interfacial tension, wettability and relative permeability.

1.2.2.1

Interfacial Tension

In the interface between two fluids molecules of one fluid are not surrounded by the same type of molecules, resulting in a difference in the forces around it. This difference in the forces at the surface generates an internal pressure, resulting in the molecules at the surface to cohere more strongly to those associated to them on the surface. Like surface tension, can be considered a good measure for how different the two fluids are, with the interfacial tension decreasing in value with fluids with similar properties, and approach zero when the fluids are miscible. This results in the interfacial tension being of vital importance when considering the interaction between two fluids, and is commonly represented as σ .

The interfacial tension between two fluids can be modified using surfactants, with different experimental and industrial intents.

1.2.2.2

Wettability

The wettability can be considered the tendency of a fluid to spread on a solid surface. The contact angle between a drop of the fluid and the surface is most times used to evaluate the wettability of that fluid in the surface, and the lower the contact angle between the two tends to represent a better wettability between them. Most of the rocks and surfaces are more commonly divided in water-wet or hydrophilic, when the surface demonstrates more affinity to water, and oil-wet or hydrophobic, when the affinity is greater with oil (Figure 1)

As previously stated, the most common method of measurement of the wettability of a surface is the contact angle, where a drop of the fluid is placed on the surface and it's contact angle with it is measured, alternatively a drop of water can be used for a more general evaluation, with angles between 0 and 75° representing a water-wet surface and between 180 to 105° an oil-wet one, Figure 1 illustrates the contact angle measurement. Although the contact angle is the most widespread method, there

are other techniques for wettability measurement such as imbibition rates, USBM method, Amott Wettability Measurements among other.[4]

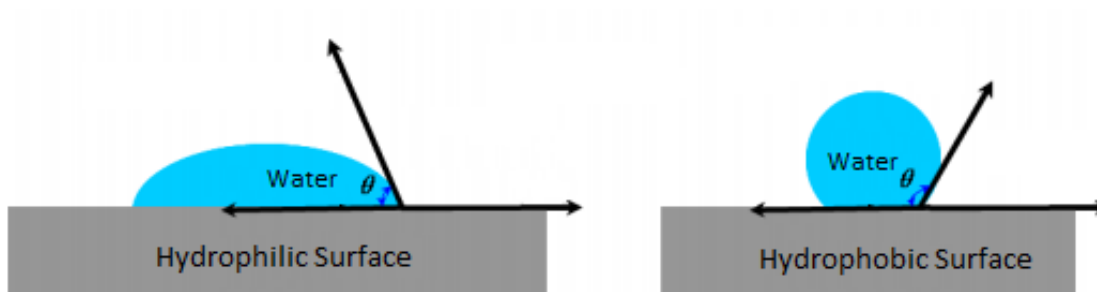


Figure 1- Contact angle between water and surfaces with different wettability. [5]

It is important to understand the wettability of porous mediums as during a multiphase flow it represents which fluid would demonstrate the tendency of flowing near the walls of the porous media. This information is key in some industries such as the oil, where the information on the wettability of the reservoir allows for the comprehension of many mechanisms in play during oil production, as well as allows for a better evaluation on which secondary and enhanced oil recovery methods should be utilized on each situation [6].

1.2.2.3

Relative Permeability

As previously stated the permeability, or absolute permeability, is a characteristic of the porous media that indicates the capacity of the medium to allow fluids to pass through it. However, when two or more fluids are flowing simultaneously they affect each other's capacity to move through the pores.

Unlike the absolute permeability, that is a characteristic of the porous media, the effective permeability is a function of not only the media, but also of the fluids properties and saturation [7].

It is more convenient to write the multiphase Darcy's equation in terms of the relative permeability, not the effective permeability of each phase. The relative permeability is the ratio between the effective permeability of a fluid and the absolute permeability of the porous media, with its values usually ranging between 0 and 1. The relative permeability is affected by the phase saturation in the porous media, the wettability of each phase, as well as the saturation process (drainage or imbibition), and is usually presented in the form of relative permeability curves, shown in Figure 2.

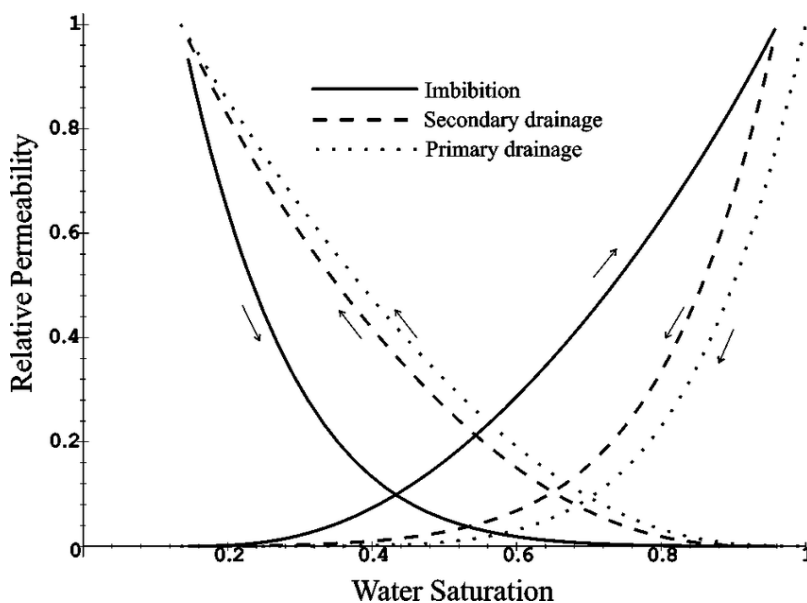


Figure 2- Relative permeability curves on the left with the drainage process and in the right the imbibition process.[8]

In the example above (Figure 2), the curve in the left is the relative permeability of the oil and the one in the right of the water, and the porous media was water wet. The curves show that the relative permeability reach a value of 0, meaning no flow in the system, with saturations different then 0, indicating that there are volumes of the fluid that cannot be mobilized, and that volume is known as irreducible saturation.

This irreducible saturation and the residual saturation refer to the volume of the saturating phases that cannot be further mobilized during the multiphase flow. Both unrecoverable saturations are phenomena that arise from the high capillary pressure necessary to mobilize fluids in thin capillaries and the fact that during an immiscible flow of two fluids in a porous media at low saturations the displaced phase becomes immobile [9]

Considering the above, Darcy's Law is modified for multiphase usage. where the equation becomes:

$$v = - \frac{k_{rf} \cdot k_{ef}}{\mu_f} \frac{\Delta P}{L} \quad (2)$$

With the main distinction being that the equation should be utilized separately for each fluid and instead of the absolute permeability of the porous media, the relative permeability of each fluid is the parameter utilized for their apparent velocity calculation. In this equation k_{rf} represents the relative permeability of the fluid and k_{ef} the fluids effective permeability, with ΔP representing the pressure drop.

Additionally, a widely used relation used in the oil industry for two-phase flows in a porous media with the injection of aqueous fluids in the reservoir is the Capillary number. Figure 3 shows a graphic presenting the relation between the capillary number of the injected fluid and the residual oil saturation for different viscosity ratios between the receding fluid and the invading one. The capillary number is a dimensionless number that represents the balance of the viscous forces (velocity and viscosity) in comparison to capillary forces (interfacial tension) in a determined flow, it is calculated as:

$$Ca = \frac{\mu v}{\sigma} \quad (3)$$

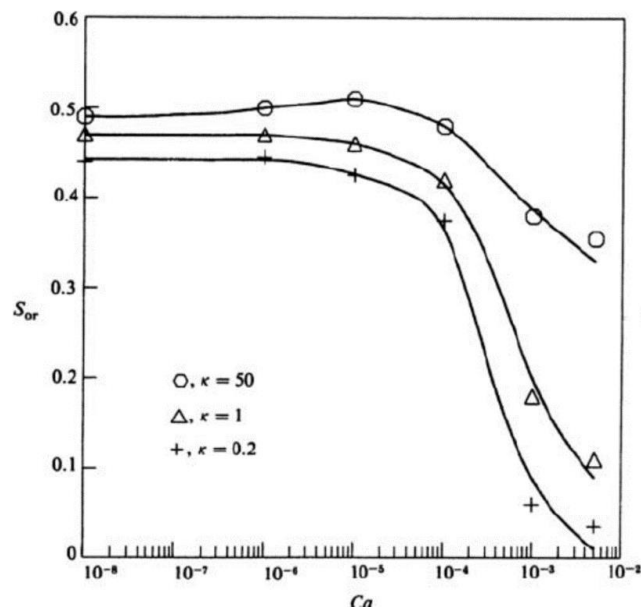


Figure 3- Residual oil saturation variation with the injecting capillary number for different permeability [10].

The curves show that for lower capillary numbers of the displacing fluid the residual oil saturation suffers little to no effect with the change in the capillary number but for higher values, an increase results in a considerable increase in the oil recovery. Also demonstrates the importance that the viscosity of the injected fluid in the recovery process as higher viscosity ratios present a smaller improvement with the higher values of capillary number.

1.2.3

Flooding as an EOR Method

Flooding is a process used after the initial stages of oil recovery with the intent of prolonging the lifespan of the reservoir. It consists in the injection of a fluid in the reservoir through one or more injection wells. Distinct fluids are used with different intents, but primarily to reduce the pressure drop due to depletion of the reservoir, by supplementing it with energy by the injection of the fluids, as well as physically displace the oil into one or more production wells, with the fluid being chosen

depending on reservoir conditions [11]. In this work the focus will be on water flooding and emulsion flooding

1.2.3.1

Water flooding

Water flooding is the most common method of secondary recovery in the oil industry, being widely used worldwide for its low cost and easy accessibility of water for the injection. The process acts similarly as a water drive reservoir, which are reservoirs that are bounded by an aquifer[12]. Besides mitigating the pressure drop in the reservoir, water flooding may also improve the oil recovery through physical displacement of the oil that is left in the pores of the rock by the injected water, though the efficiency of such displacement is variable and dependent on different characteristics of the porous media and fluid properties.

Water flooding is a long process that can go through decades, requiring periodic monitoring of field production and pressure data, for an evaluation of its efficiency. The effectiveness of a water flooding project in a given oil field depends on a number of aspects, but most importantly, the mobility ratio between the oil and the water, the geology of the reservoir and its wettability.

The mobility ratio is the ratio between the mobility of the water and oil phase, in reservoir conditions. The mobility of a fluid represents how easily it can move through the pores and create preferential paths in low resistance areas, making this an important aspect to be taken under consideration during the water flooding process [35]. The mobility ratio is represented as:

$$M = \frac{\lambda_w}{\lambda_o}, \quad \lambda = \frac{k_e}{\mu} \quad (4)$$

Where λ_w and λ_o represents the mobility of the aqueous and oil phase respectively. The mobility of a phase is considered as ratio between its effective permeability (k_e) and viscosity (μ). For water flooding, the mobility ratio usually is

higher than 1, due to the low viscosity of the water, leading to a phenomenon called viscous fingering.

In viscous fingering, water, moving through the more viscous oil phase creates preferential paths affecting the sweep efficiency of the water flooding, as the water quickly reaches the production well with a considerable section of the porous media untouched by it [13]. Porous mediums with a more homogeneous pore distribution, although still susceptible to this effect, are usually less affected by the formation of the preferential paths of the water [14]. Figure 4 illustrates the viscous fingering formation.

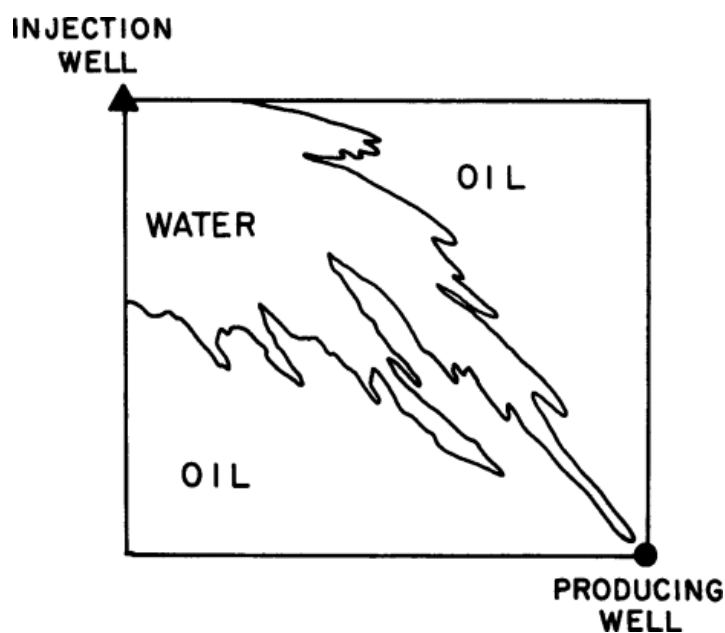


Figure 4- Viscous fingering in a water flooding. [36]

As reservoirs are heterogeneous formations, a study of the rock condition is vital for a successful water flooding project, because some heterogeneities may directly affect the injection of water in the system. So before a water flooding can be performed it must be assessed the level of heterogeneity of the rock as well as to determine its nature, paying special attention to any impermeable layer or fracture, which may exist between the production and injection wells.

1.2.3.2

Emulsion flooding

Emulsion flooding is an enhanced oil recovery process that consists in the injection of an O/W dispersion, usually performed in a process known as water alternate emulsion (WAE) where an emulsion flooding occurs between two water floodings.

The injection of controlled emulsions can be beneficial to oil displacement due to the physical interactions with the porous media and mobility control that is associated with the flooding. During emulsion flooding, the dispersed phase of the emulsion leads to a blockage of pores as they flow through it, and these blocked pores may prevent the water from flowing through the previously created preferential paths. With the established preferential paths blocked by the dispersed phase of the emulsion the water is forced to go through different areas of the porous media resulting in a better sweep efficiency of the posterior water flooding. Figure 5 illustrates how the pore blockage works.

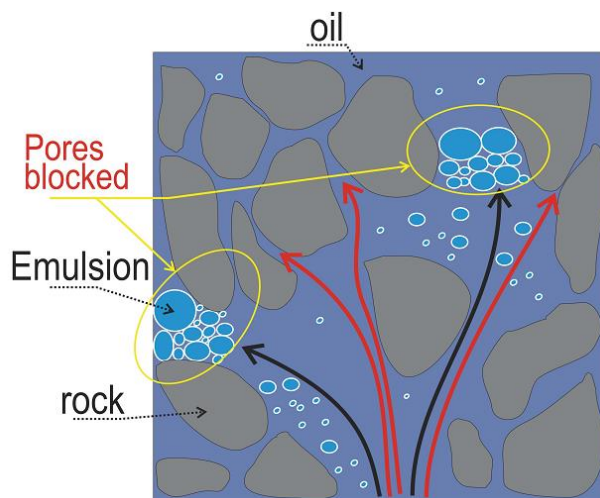


Figure 5- Illustration of pore blockage during emulsion flooding, altering the preferential paths of the water.[15]

As the image illustrates the initial preferential paths created during the water flooding, represented as black arrows, are blocked by the droplets resulting in the water flowing through different pores, represented as red arrows.

Beyond diverting the paths taken by the water during the injection, the emulsion flooding also positively affect the oil recovery with an increase in the pressure around an oil ganglia, due to the blockage of pores in its proximity. With this increase in the local pressure around the oil ganglia may surpass its capillary pressure resulting in its mobilization [16].

1.2.3.2.1

Emulsions and surfactants

Emulsions is a type of dispersed system composed of two immiscible fluids, insoluble in each other, with one of them dispersed, commonly in the form of droplets, called the dispersed phase, in a continuous phase of the other fluid. Simple emulsions, emulsions composed of two phases such as the one used during our experiments, tend to be classified as oil in water (o/w), represented by an organic dispersed phase in an aqueous continuous phase, and water in oil (w/o), when the dispersed phase is the aqueous and the continuous is organic, Figure 6 illustrates these classification.

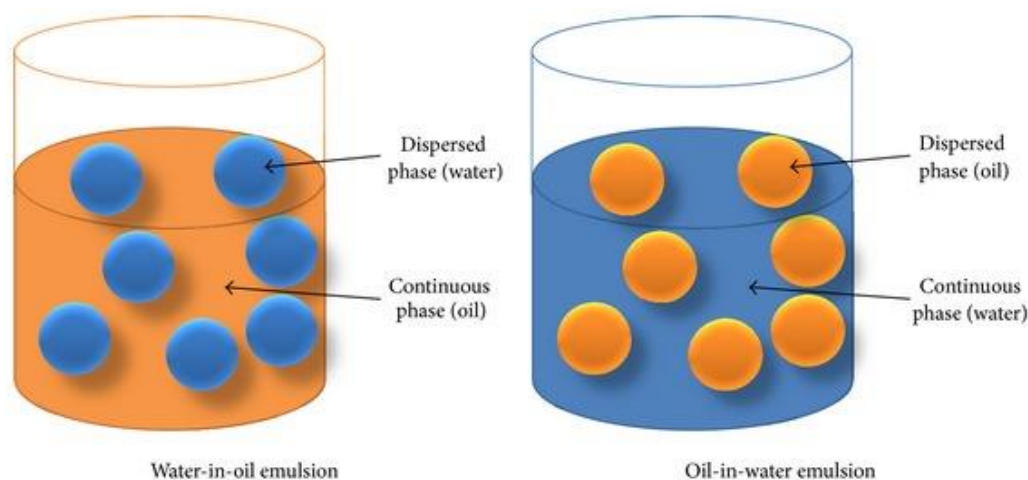


Figure 6- Two phase emulsions. [17]

Emulsion formation occurs when energy is applied to a system of two immiscible fluids in order to deforms the interface between them, generating the drops.

The increase in the total interfacial area with the formation of the droplets, results in a high energy requirement for the process. To mitigate this effect, adding a surfactant to the system results in a decrease in the interfacial tension between the two phases, what in turn reduces the energy required for the emulsification process [18].

Surfactants, also known as surface active agents, are molecules, usually of organic nature, that are amphiphilic, they have one part being hydrophilic and one part hydrophobic, commonly the hydrophobic part consists of an alkyl chain and are one class of emulsifiers, making a droplet stay in the continuous phase for a longer time without coalescing.

By its dual nature, the molecules tend to accumulate in the interface of the continuous and dispersed phases, partially submerged in each phase creating an energy barrier towards the agglomeration of the drops, which is the precursor for most of the destabilization mechanisms [19]. Figure 7 exemplifies an emulsifier.

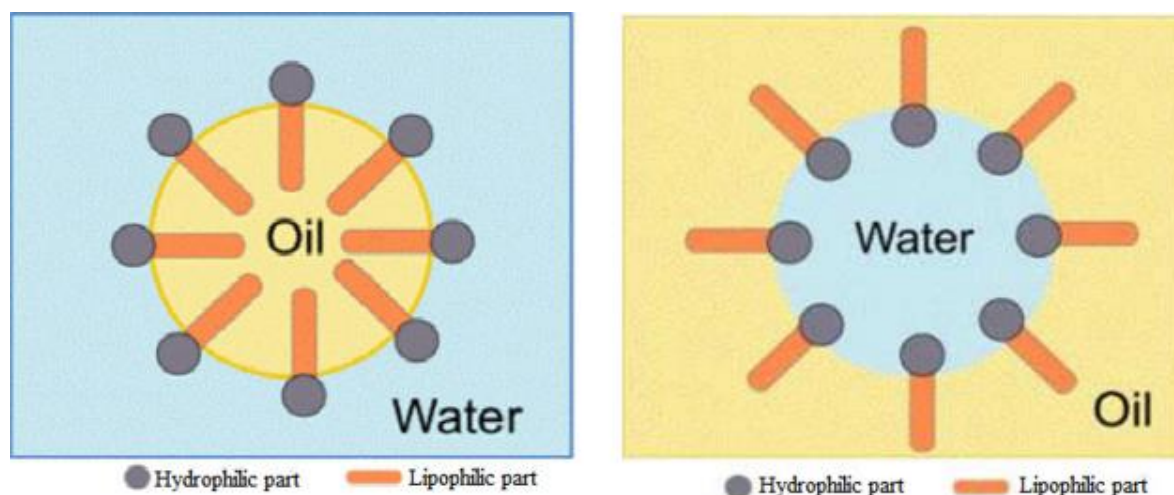


Figure 7- Surfactant in emulsions. [20]

Surfactants are divided in 4 main groups based on their electrical charge. They can be Anionic, Cationic, Nonionic and Amphoteric.

Anionic surfactants possess a negatively charged hydrophilic group, usually sulfate, carboxylate and sulfonate, with a metal, normally an alkali one, that dissociates

as a cation in water resulting in a negatively charged surfactant. Anionic are the most commonly used surfactants, representing approximately 50% of the surfactant production.

When a surfactant is initially added to a solution it will initially cover the surface of the solution, until the surface is saturated with surfactants and the monomers in the solution start forming micelle, this surfactant concentration is called Critical Micelle Concentration (CMC). The CMC is defined as the concentration at which the surface between the fluids is completely saturated with surfactant and micelles, colloidal sized association of surfactant molecules, start being formatted in the bulk and any further addition of surfactant to the solution will result in further micelles without any effect in the surface between the phases. The interfacial tension decreases with the adsorption of the surfactant in the surface of the fluids, but as the critical micelle concentration is reached, the interfacial tension stabilizes and do not vary with further addition of surfactant, Figure 8 illustrates critical micelle concentration and the surface tension variation with the concentration of surfactant.

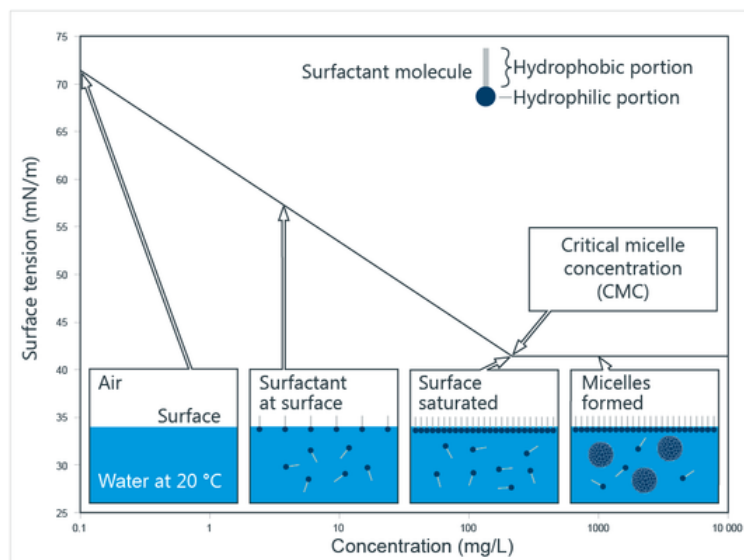


Figure 8- Surface Tension variation with surfactant concentration, and illustration of micelle formation on the CMC. [21]

The chosen surfactant also has a great influence in the determination of the continuous and dispersed phase of the produced emulsion, independent of the volume of each phase [22].

1.2.3.2.2

Emulsion formation and characterization

The characteristics of the emulsion, such as the size of the drops and which phase will be the dispersed one, depend on many parameters such as the mechanical energy, volumetric ratio between phases, presence of impurities or surfactants, degree of dispersion but also on the method of preparation, leading to formulas that work in one place generating different results in another, as apparently negligible details cause big effects. This is one of the main reason for the complexity of realizing experimental studies with them [23].

The energy necessary for emulsion formation may be transferred for the system through a number of ways, one of the most common ways being through mechanical energy, such as with the usage of a stirrer. However, some of the methods of emulsion formation may result in drops with high polydispersity in their sizes, the formation technique that allows for some of the best control in the size and monodispersity of the droplets it is through microfluidics. With microfluidics the emulsion is created with the fluids being injected perpendicularly in a constriction or flow focused, with specific combinations of flow rates resulting in different drop sizes [24].

A few aspects directly influence the stability of an emulsion such as the size of the droplets and its concentration, viscosity of the continuous phase, interfacial properties (interfacial tension and interfacial rheology), temperature as well as the aging of the emulsion.

With emulsions of oil in water (O/W), which will be the focus of this study, the most commons causes for instability are derived from coalescence, the process where two or more drops merge during contact resulting in a single drop, and flocculation,

where the drops form an aggregation in a 3D cluster without coalescence occurring [25]. These instabilities can result in a phenomena called creaming, a process that is not a breaking of the emulsion per se, but a separation of it in two emulsions, one, the cream, that is richer in the disperse phase than the other [26], Figure 9 represents these instabilities processes. Creaming is problematic as this separation may result in further coalescence, due to the proximity of the drops in the cream, or in emulsion inversion, where the phase that used to be the dispersed becomes the continuous and the phase that use to be continuous becomes dispersed. It is important to notice that, for emulsions stabilized through the usage of surfactants, the energy barriers obtained experimentally are usually very high, resulting in a prevention from flocculation, which can be explained through the repulsion between the surfactant particles [18].

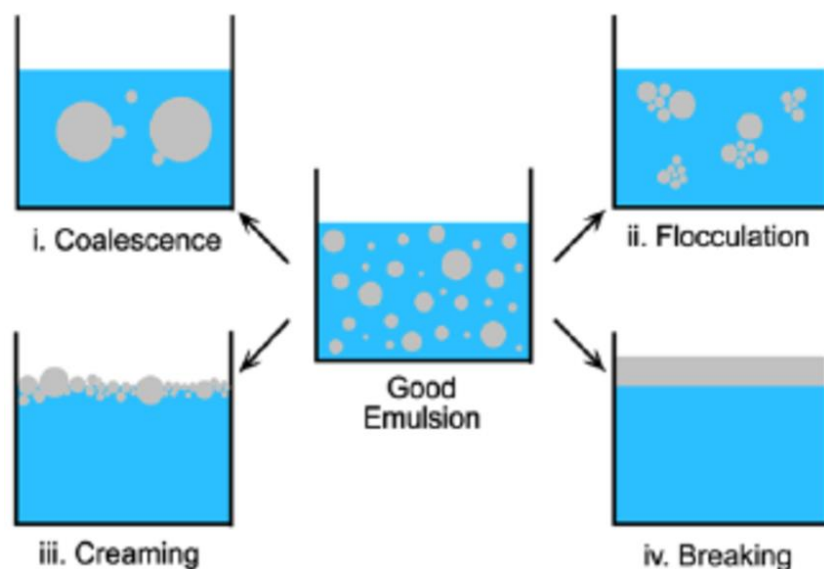


Figure 9- Schematic representation of instability process in emulsions.[27]

Depending on the size of the dispersed phases, emulsions are classified in two groups. Microemulsions, which have an isotropic dispersed phase and drops ranging in size between 1 to 100 nm in diameter, usually from 10 to 50 nm. Can also be macroemulsions, a system where the dispersed phase is composed of drops ranging between 1 to 100 μm in diameter. All the emulsions utilized during this experiment were macroemulsions.

Macroemulsions are thermodynamically unstable, that is to say that the emulsion, given enough time, which can vary from seconds to a few hours, will tend to reduce its free energy by reducing the total interfacial area, resulting in an increase in droplet size that will ultimately lead to the separation of the emulsion in the two immiscible fluids used during its production [18].

As stated in the previous paragraphs, emulsion production can be performed through a multitude of procedures based on the energy utilized during the emulsification process. During this current work the main focus of studies will be on the emulsion production via microfluidics.

1.2.3.2.2.1

Emulsion Production in Micromodels

For the emulsions used during the experimental procedures of this study, the process that we decided on for their creation was to perform it with microfluidics through a focused flow mechanism, using a micromodel with a T-junction. This low-energy methodology was chosen for the emulsion formation in the performed experiments due to the high controllability that it gave us in the emulsion size dispersity.

The drops formed with the T-junction are created due to the pressure generated by the cross flow in the junction, which results in cutting forces. As the droplets are formed due to the forces from the flow, their characteristics are heavily influenced, and can be controlled, by the ratio between the flow rates of the dispersed and continuous phases, the viscosity of the continuous phases and the geometry of the micromodel being utilized [24], [28]. As a result of their dependency on such factors and the capacity to control them with certain precision, the emulsions produced with these methods commonly present a high uniformity ratio among the disperse phase and are monodisperse [28].

The droplet formation in a T-junction can happen in one of three distinct regimes. These different regimes are squeezing, dripping and jetting and the drop

formation mechanisms in each of the regimes differs from one another, resulting in with similar conditions, each of them produces droplets with distinct characteristics.

The squeezing regime presents as its predominant force the interfacial force. The dispersed phase drop invades the main channel and almost fills it in its entirety, causing the continuous phase to be confined in a thin film between the invasion fluid and the channel wall and resulting in an increase in the pressure behind the forming drop. With the build-up in the pressure the neck of the dispersed phase is compressed until it is severed and the drop is formed. In this regime the drop size, which usually is considerably bigger than that of the channel, is governed by the flow ratios between the dispersed and continuous phase and usually happens with low capillary number [24], [29]. Figure 10 illustrates this regime.



Figure 10- Emulsions being formed through squeezing, the dispersed phase presented as orange and the continuous phase as blue [29].

The jetting regime is symbolized by the presence of a long filament of the dispersed phase that invades the main channel near the wall with a laminar flow parallel to that of the continuous phase with a length significantly larger than its width, resulting in the droplet formation occurring after the junction. This mechanism is produced as a result of the inertial forces in the dispersed phases overpowering the interfacial forces, culminating in the formation of the invasion jet which eventually breaks in droplets [24], [29]. Figure 11 illustrates droplets being formed with this mechanism.

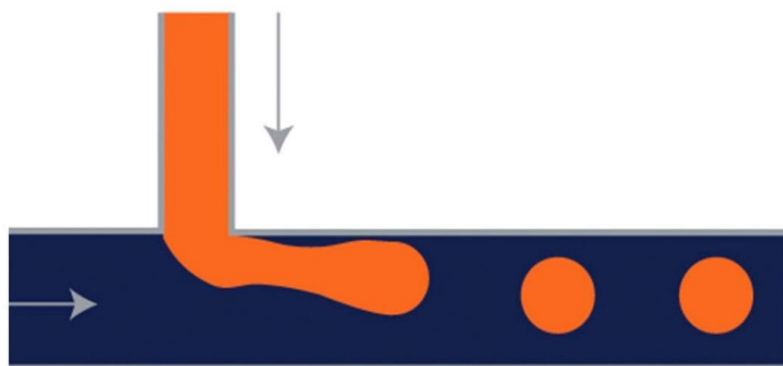


Figure 11- Emulsions being formed through jetting, the dispersed phase presented as orange and the continuous phase as blue [29].

In the dripping regime the interfacial forces pull the dispersed phase back in the injection channel during the droplet formation, with the dispersed phase being unable to properly invade the main channel, leading to the drops to be created close to the injection capillary. In this formation mechanism the size of the formed droplet is dependent on the capillary number. Figure 12 illustrates the dripping regime for emulsion formation.

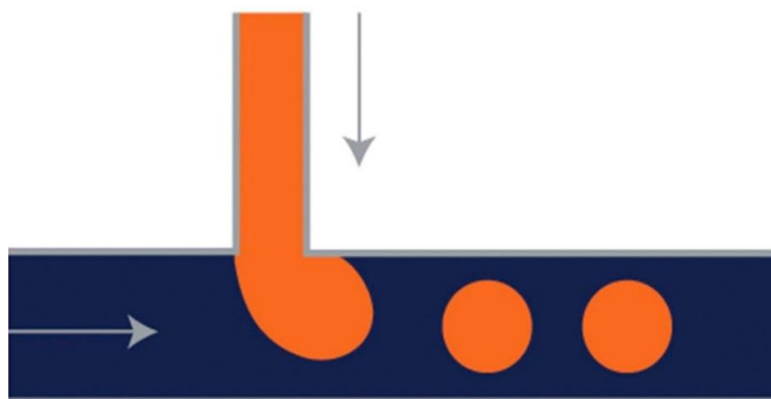


Figure 12- Emulsions being formed through dripping, the dispersed phase presented as orange and the continuous phase as blue [29].

1.3

State of Art

McAuliffe (1973) performed one of the first studies centered on the utilization of emulsion flooding as an enhanced oil recovery mechanism. He demonstrated that the injected emulsion could perform a selective blockage in the pores along the preferential paths of the water, leading to a better sweep efficiency and oil recovery in subsequent water flooding. His results demonstrated that the drops of the emulsion resulted in a reduction of permeability in the areas where the blockage occurs, and that such reduction is sustained even after larger volumes of water are injected in the porous media. His experiments also demonstrated that the injection of a particle of the same size or slightly bigger than the pore results in a higher efficiency [30].

Schmidt et al. (1984) performed an experimental analysis of the injection of stable emulsions as a method for oil recovery. The performed experiments indicated a capacity of the injected emulsion to reduce the mobility of the aqueous phase after the oil droplets are captured in the pores of the porous media, acting as a filtering process. The study also determined that the emulsion injection was also capable of changing the preferential paths of the water phase, presenting positive effects not only in linear mobility control but also in diverging the flow to areas of the porous media with low permeability. The authors also presented two distinct parameters that are vital for the effectiveness for an emulsion flooding a drop penetration and permeability reduction capacity, but these characteristics are inversely related. Larger drops produce a high permeability reduction during their injection are retained by the medium easily which results in a low penetration, in contrast smaller emulsions can flow through and penetrate more easily the porous media but do not effectively reduce the permeability of the aqueous phase, with both scenarios resulting in less than optimal oil recovery. Through these data it was suggested that an intermediate sized emulsion would result in better results for oil recovery as it would possibly present a better penetration in the porous media with the permeability reduction.[31].

Bryan et al. (2009) utilized an experimental approach backed by numerical validation to study the effects of emulsions in oil recovery. During their studies the

emulsion was formed inside of the porous media, instead of being injected in it, through an alkali flooding with the surfactant generated in-situ as a result of the interactions of the alkali with the organic acids, this way producing the dispersed phase. The experiments demonstrated that after the emulsion formation there is a pressure build up in the system along with an increase in oil production and a reduction in water production. The results presented that the emulsion formation in the reservoir not necessarily results in a reduction in the residual oil saturation in heavy oil scenarios, with the emulsion formation accelerating the oil recovery but not necessarily increasing it [32].

Cobos et al. (2007) studied the behavior of the emulsion with droplets of two different sizes flowing through a constricted capillary. The work demonstrated that when flowing through a constricted capillary drops with a size similar to the constriction presented a better blockage, resulting in a bigger pressure drop in these scenario. The experiments also demonstrated that in lower flow rates the blockage of the pores by the disperse phase is more effective, as in higher flow rates the effect of the forces of the flow makes more difficult for the drops to block the pore [33].

Guillen et al. (2012) studied the effects of WAE in additional oil displacement through different experiments. An experiment with an unconsolidated porous media, composed of glass spheres for a visualization in pore scale, demonstrated an increase in the pressure during the emulsion flooding and demonstrated an alteration in the preferential paths of the water due to the blockage of the pores by the disperse phase of the emulsion, resulting in an increase in the oil recovery in the system. Another experiment conducted with sandstone cores of different permeabilities in parallel resulted in a reduction in the mobility in the core with higher permeability resulting in a ratio of mobility between the two cores reduced and as a result in the water flooding also displacing oil from the lower permeability core.[34]

Moradi et al. (2014) performed experiments to study the usage of emulsion flooding as a mechanism for enhanced oil recovery. Their results indicated a better sweep efficiency of the water flooding after the injection of the emulsion, resulting in superior oil recovery. An analysis of the pressure during the experiments, indicated a

fluctuation of the pressure that was correlated with the blockage mechanism of the drops, associating it with their passage through the pores. The pressure analysis also indicated a reliance of the blockage mechanism on the capillary number, with higher flow rates the drops blocking the pores would be released at higher rate, diminishing their efficiency, and indicated that a critical capillary number, below which the drops act as an efficient mobility control agent, vary with the size of the injected drop. Though should be noticed, that during their experiments the volume of injected emulsion was of one pore volume, hence their oil recovery with such methods would not be financially viable [35].

Baldygin et al. (2014) conducted experiments developed the water alternate emulsion (WAE) mechanism for oil recovery and tested it in a core flooding in a laboratory utilizing three different slug ratios during the experiments. The experiments performed by the authors presented water alternate emulsion as a viable option for mobilization of residual oil after water flooding, presenting further recovery of at least 20%. The results of the experiment also presented some interesting results such as a separation of the emulsion inside the porous media, with the disperse phase of the emulsion being concentrated near the entrance of the core flooding [36].

Farias et al. (2016) through experiments in 1D and 3D flow configurations tested the usage of emulsion flooding as an EOR method and for mobility control. The experiments demonstrated a gain in the oil recovery due to the emulsion flooding, generating recovery in macro and microscales, and the parametric analysis indicated that an emulsion with its parameters controlled and designed for the specific scenario results in a better mobility control and subsequently oil recovery.[37]

Perazzo et al. (2018) studied single droplet and emulsion injection in porous media observing its different utilizations as well as aspects that affect them. Concerning the utilization of microemulsions for oil recovery purposes, the main drawback presented were the high amount of surfactant necessary for the formation, but presented new developments with the combination of amphiphiles with large head groups and long tails with nonionic surfactants for a boosting in emulsion formation with less volume of surfactant required, and suggests experiments with different combinations

of surfactants and co-surfactants at different salinity levels for further reduction of its surfactant concentration [38].

1.4

Objectives

Our main focus is to visualize and comprehend the pore-scale effects of an emulsion flooding in the residual oil saturation in a porous media. In order to better understand the effects of the properties of the dispersed phase of the emulsion in the oil recovery it is also our intent to draw a parallel between the size of the droplets and the residual oil saturation in the porous media. It is also of our intention to understand and analyze the correlation between the injection flow rate, and the capillary number, with the volume of recovered oil during the emulsion and water flooding.

We also seek to understand and observe the blockage mechanisms and the behavior of the droplets during the injection. This will also englobe an analysis of the droplets distribution along the porous media after the ending of the injection and an evaluation of the size of the drops along the porous media to better comprehend the effects of the pores and pressure in the structural composition the disperse phase of the emulsion.

2

Experimental Approach

In brief, the experiment consists in a water flooding conducted in a glass micromodel that is completely saturated with oil, which acts as the porous media. With the water flooding completed after the injection of two pore volumes, approximately 75 μ l, and emulsion is produced using another microfluidic device to be subsequently injected online in the porous media at the same flow rate as the water flooding. After the emulsion injection is ceased images of the porous media are taken and subsequently treated to calculate the volume of oil still in it.

This section of the work will explain further the experimental procedure utilized in this study as well as the associated equipment. For an easier comprehension of all the steps of the experiment during the explanations the experiment will be divided in its two large section: Emulsion Production and Flooding.

2.1

Material and Methods

For the success of the experiment, it was essential the utilization of a series of equipment and materials that had specific characteristics. For an easier understanding, this equipment can be divided in a few groups due to their role in the experiments.

Formation Micromodel – A glass micromodel with a T-junction used for the emulsion formation.

Porous Media Micromodel – A glass micromodel composed of a random distribution of pores and channels, which acts as the porous media for the experiments.

Injection System – The fluid injection system utilized for the saturation and flooding performed in the experiment. Composed by two syringe pumps and syringes.

Solutions – The fluids used during all the steps of the experiment. Being an aqueous solution and an oil.

Image Acquisition and Analysis System – The components used during the data acquirement and processing for the experiment. Formed by an inverted microscope used to take pictures of the porous media device after the flooding and a computer with the ImageJ software for the evaluation of phase distribution.

These groups and equipment will be further explained in details in this following section.

2.1.1

Micromodels

Two different micromodels were used during the experiments. Both micromodels present a few advantages that made us choose them for the experiments, such as the fact that it has simple channel geometry, allowing for a high production rate and extremely consistent droplet size. The micromodel has a high visibility, being ideal to work with a microscope, and a good chemical compatibility with the working fluids, not reacting with anything during the experiments, and it also has a wide temperature and pressure work range. The channels also do not suffer deformations, thermal or mechanical, which can happen with other devices [39].



Figure 13- Connector utilized in the devices/ Datasheet

Both micromodels work with a specific connector, shown in Figure 13, a Linear Connector 4-Way. The porous media device uses one connector and the emulsion production utilizes two. The Linear Connector 4-Way allows a reliable connection between the Dolomite's microchips and 1.6 mm O.D. tubing, connecting in the top surface of the chip. It has the benefits of having low dead volume ($<0.1\mu\text{l}$), being quick and easy to connect and disconnect and having a wide pressure and temperature range. The connector permits the usage of up to 4 tubing at the same time

2.1.1.1

Emulsion Formation Micromodel

For the creation of the emulsions utilized during the experiments, it was utilized the "T-Section" of a Droplet Junction Chip, shown in Figure 14. The chip is commercialized by Dolomite Microfluidics, made in glass, carved with hydrofluoric acid, and bonded through a thermal treatment.

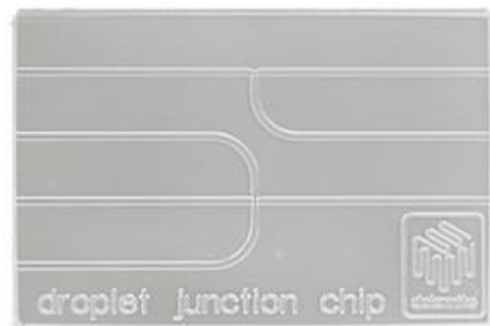


Figure 14- Droplet Junction Chip made by Dolomite/ Datasheet

It was decided to employ the micromodel for the creation of the emulsion drops, as one of the focus of our study was to and better understand the effects of the drop size during the experiment, and using microfluidics it would be easier to could control the sizes of the drops and assure of its monodispersity.

The T-Section has two inputs and one output channels, with a depth of $100\mu\text{m}$ and a width of $300\mu\text{m}$, while the junction has a $100\mu\text{m}$ depth with a $105\mu\text{m}$ width, Figure 15 presents a schematic image of the device with a zoom in the T section. In order to create drops, the oil was injected in the bottom channel while the aqueous solution was injected through the left channel.

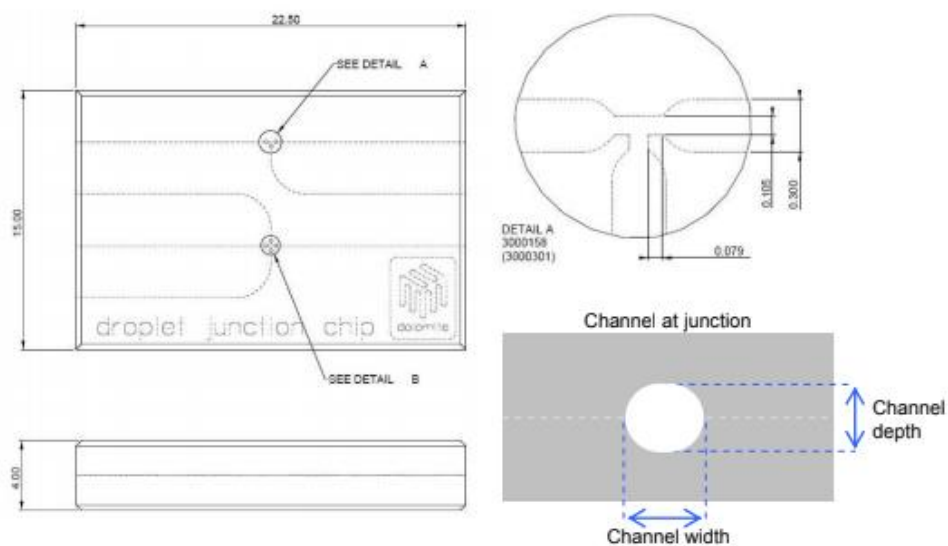


Figure 15 – Schemed image of the microfluidics device used for the emulsion formation, with focus in the T-Section./ Datasheet

As the glass surface of the channel is naturally hydrophilic, it is ideal for the formation of organic droplets in a continuous aqueous phase, as it is desired for our experiments. If it becomes necessary the formation of an aqueous drop in a continuous organic phase, it would be required a hydrophobic coating in the channels of the device.

After each experiment the micromodel is cleaned and emptied of all the fluids by the injection of high pressurized carbonic gas.

2.1.1.2

Porous Media Micromodel

A Porous Media Chip, also made by Dolomite Microfluidics, shown in Figure 16, was also utilized during our experiments. This microfluidics device acted as the porous media for the purpose of our experiments, modelling complex porous rock structures, allowing us to better analyze and observe the displacement of the oil due to the water and emulsion flooding.



Figure 16- Porous media device./ Datasheet

The Porous Media Chip is made in glass, carved with hydrofluoric acid and attached with a thermal treatment. The micromodel presents a few advantages such as a broad temperature and pressure working range and high visibility of its channels, allowing for the visualization at a microscope of all of our fluids. Figure 17 presents a schematized view of it,. During our experiments the channels in the utilized Porous Media Devices were waterwet, as to not have any possible effects of difference in wettability affecting the results.

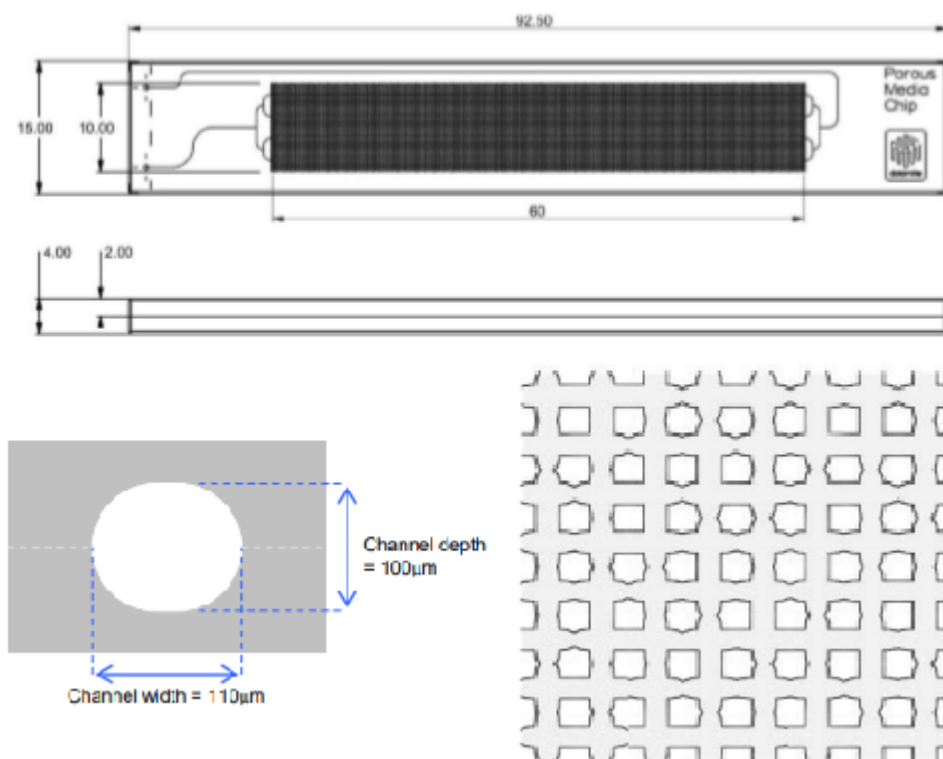


Figure 17- Schematic view of the porous media device./Datasheet

The channel of the porous media device is 100µm in depth with 110µm width. The absolute permeability is 79 D, porosity 0.32 and volume of the entire porous media is of 38µl, in an area of 60mm width and 10mm depth, where the microchannels are interconnected. The micromodel has one entrance and one exit, and to ensure that the flow will be equally distributed through the porous media both the entrance and the

exit are divided twice, resulting in 4 points of access and 4 points of output in the porous area.

In order to better act as porous media for the experiment, the throats have different sizes of constrictions, randomly distributed along the porous area of the device. The throats can be constituted by constrictions, which can be of $63\mu\text{m}$ or $85\mu\text{m}$, and channels, of $110\mu\text{m}$. The grid is composed of this randomized pattern of 8 throats width for 8 throats depth ($2 \times 2 \text{ mm}$), shown in Figure 18, that is repeated throughout the whole length of the porous media, a total of 150 times. This pattern has 38 constrictions of $63\mu\text{m}$, 40 of $85\mu\text{m}$ and 50 channels of $110\mu\text{m}$.

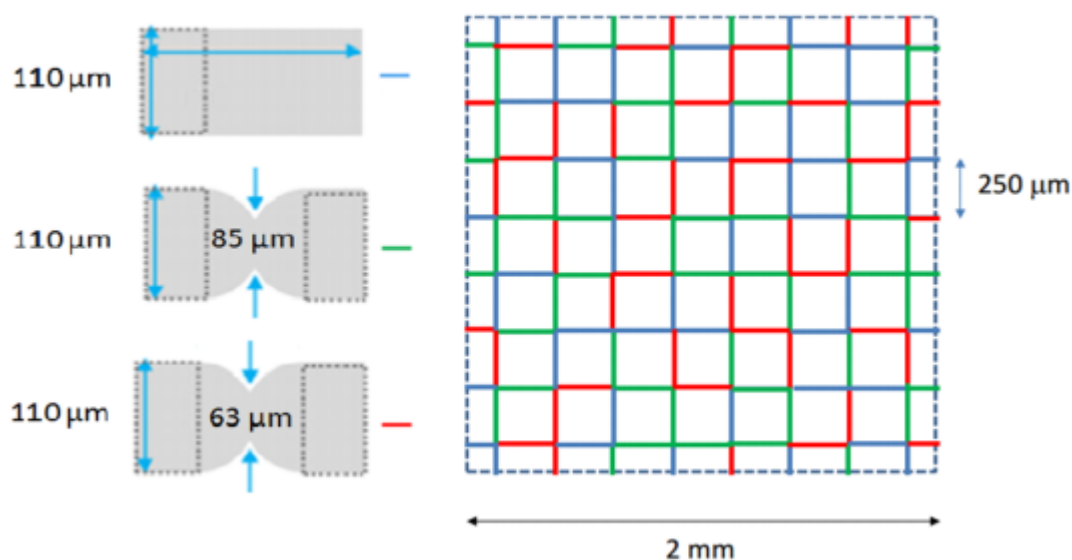


Figure 18- Randomized pattern of channels and throats repeated in the porous media./ Datasheet

During the experiments the micromodel is maintained in a plane horizontal surface to minimize the gravitational effects during the flooding and to not interfere with the preferential paths of the water.

After each experiment it is of vital importance for the micromodel to be properly cleaned, as any impurity may result in a difference in pressure that can greatly affect the results of the experiment, so a cleaning protocol was determined to minimize the odds of such and external interference to occur.

With the conclusion of each experiment, after the acquisition of the images post emulsion flooding are taken, the micromodel is connected to an air exit where carbonic gas at a pressure of 90 psi is injected in the porous media for 30 minutes with the intention of remove most of the fluids that are saturating it. After the gas injection the micromodel is connected in a syringe with ethanol that is injected with alternating rates, starting with 6 ml/h and increasing until 12 ml/h, until all the other fluids have exited the porous media and it is completely saturated with the alcohol. With the porous media completely saturated with ethanol the connector of the micromodel is removed the microchip is then taken to a heater at 100°C for 45 minutes for the complete evaporation of the alcohol. Afterwards the emptied porous media is left cooling down, at room temperature, before being plugged again in the connector, and being ready for a new patch of experiments.

2.1.2

Injection System

The fluid injection system for the experiments were composed of two pumps and a set of syringes, that were utilized for the injection of different fluids into our system, with each syringe being utilized with the same fluid in all the experiments. The same pumps, connections and syringes were utilized during every experiments, to avoid possible influences that the change in equipments could have in the results.

The syringe pumps used during the experiments were Harvard Apparatus Elite 11, shown in Figure 19. They work with syringes of a minimum volume of 0.5 μl and a maximum of 60ml. The pump controls the injected volume through the diameter of the syringe being utilized, having already programmed in its system the information of a number of syringes not being necessary for manual input of the data, minimizing the odds for a human error. This model was chosen due to its control and precision, presenting an accuracy and reproducibility of 0.5% and 0.05% respectively. The pump also provides a “lock” feature, preventing accidental changes in the system configuration, ensuring the integrity of the experiment.



Figure 19- Model of the utilized syringe pumps during the experiments./Datasheet

The pumps presented an important feature allowing the setting of a target volume or time of injection after which the pump automatically stops, this being key for our control of the volume of injected fluid in the microscopic devices and volume of created emulsions to be injected in the porous media.

All the experiments were conducted with plastic BD syringe's, with different diameters chosen depending on the flow rate required in each scenario, with the intention of respecting the table of minimum and maximum rates per size provided by the pump, resulting in a more precise flow rate during injection. The plastic syringes were chosen in view of their easy maneuverability they provide and due to the fact that none of our working fluids react with plastic, so it wouldn't be a problem.

For the connection between the syringes and the micromodel, microfluidics connectors, a "T Connector" and a 1/32" diameter semi-flexible tubing were utilized. The connection was performed in such a way as to prevent leaking, keep the integrity of the system and the working fluids and for its stability.

2.1.3

Solutions

During the experiments, two different fluids were used in the porous media device. A solution of water with surfactant and a mineral oil Drakeol7. For a better visualization of each phase during image acquisition and analysis, different colors of dye were added to each fluid. The aqueous solution was colored red, and the Drakeol7 used for the emulsion production was dyed with a black pigment while the Drakeol7 used during the initial saturation of the device was kept transparent, allowing for the differentiation between the oil initially saturating the porous media and the oil injected posteriorly.

Due to the low volume of the porous media device, and the size of its channels, any impurity injected into it with the working fluids represented a risk of clogging the pores of the device. This would be problematic for the experiment as it could result in an increase in pressure along the porous media, influencing the preferential path of the water flooding or even blocking the entrance to the porous media altogether. In order to minimize the chances of these problems occurring, any fluid that were to be injected in the porous media were previously filtered with a filtering system using a vacuum pump, with a filter of 5 μ m. Before the fluid is injected in the microchip it is filtered a second time by a filter, of 0.22 μ m for the water and 5 μ m for the oil, that is connected to the syringe filtering during the injection.

All the experiments were conducted at room temperature (roughly 25°C).

2.1.3.1

Aqueous Phase

For the experiments, the aqueous phase used was a solution of water with Lauryl Sodium Sulfate (Sodium Docedyl Sulfate). It is an anionic surfactant with a HLB number of 40 presenting the tendency to form O/W emulsions, at a concentration of 0.86g/l to help the stabilization of the system. This concentration is twice the critical micelle concentration (CMC) of the Lauryl Sodium Sulfate. The surfactant is added to

the water with the intention of coating the drops in the inner phase of the emulsion, and with that keeping them from coalescing.

For the preparation of the solution deionized water and the surfactant are weighted and then the surfactant is slowly added to the water while a magnetic stirrer mixes them at a constant speed, and the fluid is kept at the stirrer for 3 hours. The properties of the water with the addition of the surfactant are present in Table 1.

| Fluid | Viscosity (cP) | Surfactant(g/l) | Interfacial Tension Oil/Water (mN/m) |
|-----------------------|----------------|-----------------|--------------------------------------|
| Water + Surfactant | 0.89 | 0.86 | 11.07 |

Table 1- Properties of the aqueous phase used during the experiments. All properties measured for a temperature of 25°C

The addition of the surfactant in the water was proven necessary early on, for the stabilization of the emulsions produced for the experiment, otherwise, with pure water, the emulsions would quickly coalesce.

Before the effective start of the experiments an initial test was performed comparing the recovery factor in an initial water flooding at a flow rate of 0.065 ml/h between pure water and our aqueous solution of water and surfactant. This experiment demonstrated that the volume of recovered oil did not significantly vary between both situations. With the data from this test, it was decided to use the water surfactant solution during all the processes of our experiment, considering that its effects during the oil recovery could be ignored.

2.1.3.2

Oil

The oil used during our experiments was Drakeol 7, a non-aromatic clear paraffin based mineral oil. Some of the advantages in using Drakeol 7, is its low

viscosity, lack of aromatic carbons, being of easy visualization in a microscope, being non flammable, and having most of its property already known, as shown in Table 2.

| Fluid | Viscosity (cP) | Density (g/ml) | Superficial Tension (mN/m) |
|-----------|----------------|----------------|----------------------------|
| Drakeol 7 | 17.78 | 0.8446 | 28.3 |

Table 2- Properties of the oil used during the experiments. All properties measured for a temperature of 25°C.

During the experiments, the oil was used for two distinct objectives. Initially, it was used for the saturation of the porous media device, acting as the original oil in place for our experiments, and it was subsequently used during the emulsion formation, as its inner phase.

2.1.4

Image Acquisition and Analysis System

For the visualization and image acquisition of the porous media, an inverted microscope from Leica model DMi8, was used, as shown in Figure 20. All the images were obtained using the 5x magnification lens.



Figure 20- Microscope used for image acquisition./Datasheet

The DMi8 was chosen because during the initial preparation for the experiment it presented the better resolution, lighting and contrast for the 5x magnification lens, that had already been decided on as the optimal magnification for acquisition of images of the porous media device.

During image acquisition, for a better visualization and comparison between experiments, the porous media device was divided in 3 horizontal sections (names A, B and C from top to bottom) and 14 vertical ones (numbered 1 through 14 from the entrance to the exit) resulting in a total of 42 images taken after each step of the experiment. This division allow us to better comprehend after each step of the experiment the effects in different areas of the porous media and, in doing so better understand the observed phenomena.

After the acquisition of the images they are treated in a computer initially using the program GIMP2 followed by the ImageJ software. GIMP2 is used aiming for an improvement in the resolution of the images and the ImageJ allows us to up the contrast between the phases in an image and minimize the borders of the channels.

The program is also important, as with the use of macros, it allows us to differentiate the phases in each image, with the water and emulsions being colored black and the oil white. Afterwards, it is also possible for ImageJ to evaluate how much of the picture is colored black, effectively allowing us to measure how much oil is left in place after each step of the experiments.

For a better evaluation of the oil in place with this method, it was necessary to know the volume of the space between the channels, as they also appear as black in the images, and to minimize the effect of the borders of the channels and that of shadows, or any imperfection in the images, in order to calculate a volume of residual oil as close to reality as possible.

2.1.5

Emulsions

The emulsions utilized during the experiments were emulsions of oil in water (o/w) that were produced with the usage of microfluidics techniques. This method of emulsion formation was chosen because it was considered that it would result in a better control of the drop size during the creation process and it would assure us of the monodispersity of the droplets created during this process. Following this planning, the emulsions were created with the usage of the Droplet Junction Chip. With the injection of the aqueous and oil phases in the T-Section of the micromodel in specific flow rates, stable emulsions were formed, and with a variation in said flow rates it allowed us for the creation of drops of different sizes, as depicted in Figure 21.

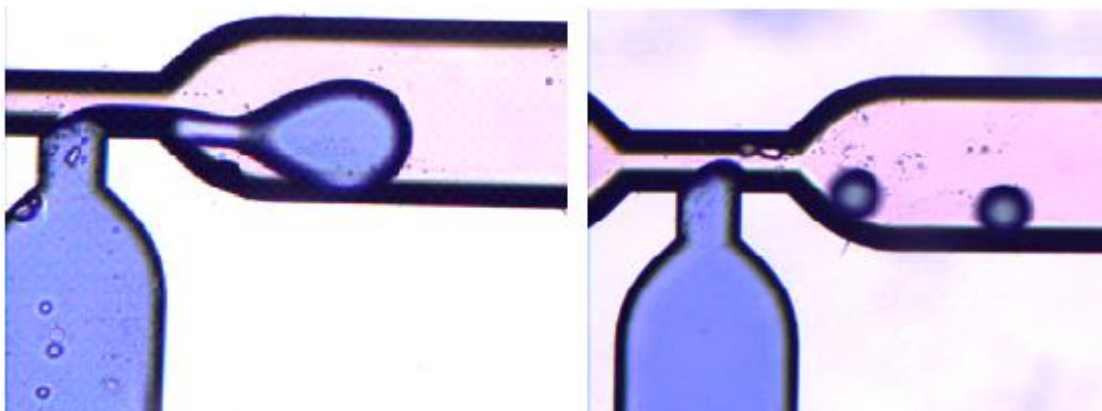


Figure 21- Process of emulsion creation, with the large on the left and the small on the right

For the preparation of the emulsion used in the experiments different combinations of flow rates of oil and water were tested, analyzing the different size of emulsions produced with each pair, before ultimately deciding on the three drop sizes that were optimal for the objectives of the experiment. The flow rates used during the creation and the sizes of the drops utilized are presented in Table 3.

| Drop Size (μm) | Water Rate (ml/h) | Oil Rate (ml/h) |
|-----------------------------|-------------------|-----------------|
| 80 | 4 | 0.27 |
| 120 | 4.5 | 0.4 |
| 175 | 5 | 0.52 |

Table 3- Formation flow rates for each size of emulsion utilized.

These three distinct sizes were decided on for the experiments as to analyze and better comprehend how the size of the injected drops would affect the volume and process of oil recovery (Figure 22). The sizes of the drops were decided based on the sizes of the porous media throats, with the intent of the larger drop being larger than the channel of the porous media and the smaller drop being larger than the biggest constriction. After initial experiments, the difference in sizes was deemed to be too big, so a third size of drop, between the two previous determined sizes, for a better evaluation of the effects of the size of the drop.

In order to avoid possible problems with the emulsions from handling and storing them, the emulsions are injected in the Porous Media Device immediately after their creation. This process, called injection in-line, permits us to be sure of the emulsion integrity as it is being injected in the micromodel and injects them in a diluted manner.

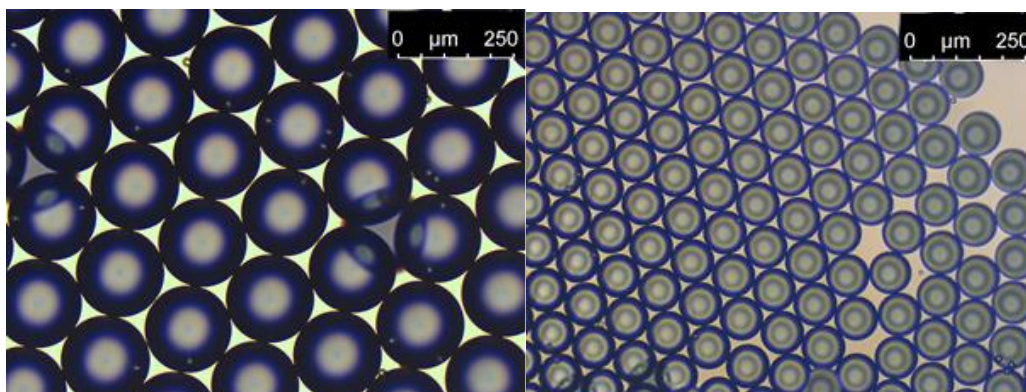


Figure 22 Emulsion droplets, largest and smallest size

The drops presented a lower density than the water, and with that, they demonstrated the tendency to move upwards during injection and movement through the tubing, which resulted in problems with the emulsions being stuck in connectors, not flowing correctly from one tubing to another and not entering the porous media. To avoid these problems, different connectors were introduced, as well as tubing of different diameters to facilitate the movement of the emulsions from one to the other, and a new vertical set-up so that the emulsions could enter the porous media more easily.

2.2

Experimental Setup

There were a few key problems faced during the idealization steps of the experiments, resulting in the necessity to develop a system configuration with the equipment that allowed for the direct injection of the emulsion after production, with this part of the experiment being identified as the most problematic one early on. After a few tests and the identification of the main problems the experimental setup was modified and optimized to better suit the needs and specifications of the project.

2.2.1

Emulsion Production

The emulsion creation through microfluidics, utilizing a T-junction in a micromodel, was something that had already been previously studied and the literature was helpful with the initial arrangement of the experimental setup. Figure 23 displays the setup utilized during the emulsion production process.

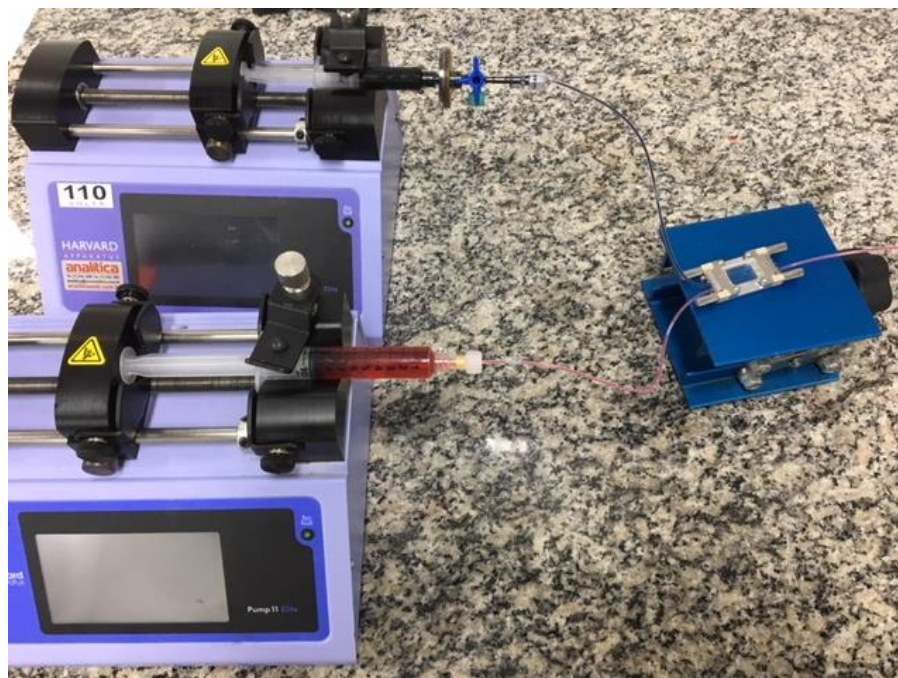


Figure 23- Experimental set-up used for the production of emulsion.

Nevertheless, a few problems arose when a method for the immediate injection after their production started to be thought of. The main difficulty came from the fact that although the idea was for the emulsion to be injected in the porous media directly after their creation the flow rates used during this process were higher than the one using in the flooding, resulting in a mobilization of most of the oil still in place in the porous media. Thus, it became necessary to keep both micromodels separated but still perform a direct injection of the emulsion after it creation.

The first problem was solved with the usage of a long exit tubing in the production micromodel. This exit tubing would be kept open to the atmosphere while the porous media device after the water flooding would be kept with its entrance and exit closed to avoid any gas from entering and compromising the results. With the desired volume of emulsion produced the oil injection in the production micromodel is ceased and the water injection reduced to the same flow rate as the one used during the water flooding. With the reduction in the flow rate of the system we wait until the exit tubing of the production device is completely saturated with water and then connect

the exit of the production to the entrance of the porous media device, taking care not to let any air into the system.

2.2.2

Fluid Injection in Porous Media

During the initials emulsion flooding tests some hindrances that we would be facing in the experiment became clear, mainly the need to assure the flow of the droplets into the entrance of the porous media device. This was made difficult due to the low density of the disperse phase of the emulsions which gave it a tendency to move upwards during flow, getting stuck in connectors and with the bulk not properly entering the device.

Figure 24 displays a scheme of the setup that was ultimately decided upon for the experiments and Figure 25 is an picture of the experimental setup assembled during an experiments.

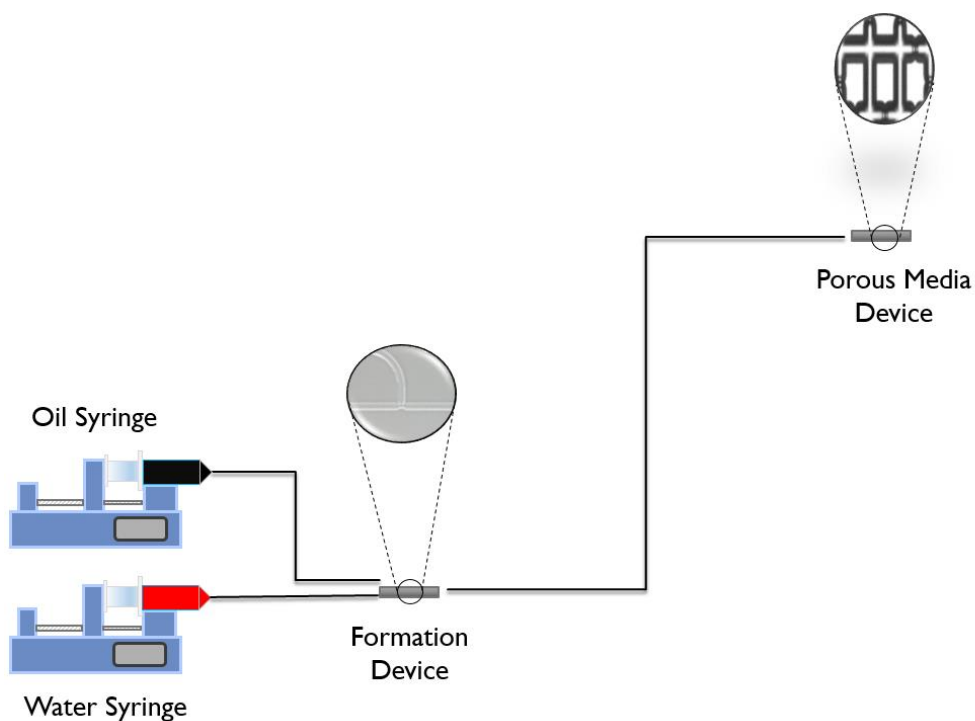


Figure 24- Schematic view of the experimental setup



Figure 25- Experimental set-up utilized during the emulsion flooding

The floating tendency of the droplets was bypassed by connecting the micromodels with a vertical distance between them. The porous media device was placed directly above the emulsion production micromodel, in a way that the liquids flowing in the tubing between them, which is kept as straight as possible, goes constantly upwards from one micromodel to the other. With this positioning, it was possible to assure an easy flow of the produced emulsion into the porous media as well as a minimization of problems arising between the droplets and the tubing connectors, as with an horizontal flow a considerable volume of the drops would get stuck in the connectors and not enter the micromodel.

The regions of micromodel are shown schematically in Figure 26.

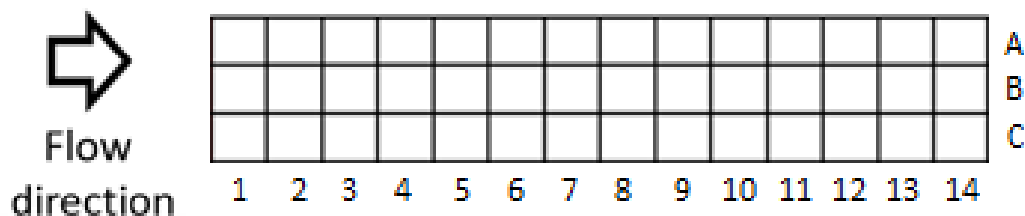


Figure 26- Regions of the micromodel.

2.3

Experimental Procedure

The experiments are initiated with the porous media clean, filled with air, and then its initial step consists with the injection of the Drakeol7 into the micromodel. The injection is started with a flow rate of 8 ml/h and then decreased to 1ml/h after the oil reaches the end of the porous media, and injection is maintained until the porous media is completely saturated with oil.

Once the micromodel is saturated with oil, the syringe with the aqueous phase is connected to the entrance tubing, keeping mind not to let any air bubble enter the system. The water flooding is than initiated and kept at a constant predetermined flow rate. Experiments were conducted using two distinct flow rates to better comprehend and compare the effects resulting from the capillary number in the volume of residual oil and in the effects of the injection of emulsions.

The water flooding is sustained until no further oil is being mobilized in the porous media due to the injection of water. Experimentally, the volume of the water flooding to reach this stage was found to be close to two pore volumes, than the flooding is ceased. With the end of the water flooding, the entrance and exit of the micromodel are kept shut keeping any air from entering it, and the device is taken to the microscope for an evaluation of phase distribution and image acquisition, Figure 27 shows the software of image acquisition.

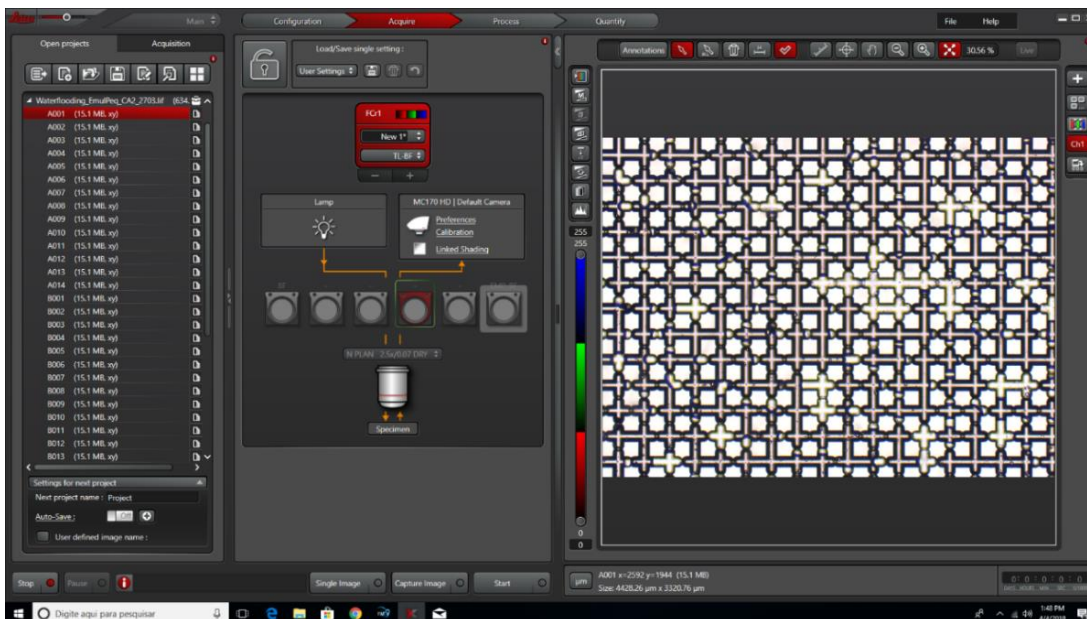


Figure 27- Software utilized for the acquisition of the images in the microscope after the experiment.

While the images of the micromodel post-water flooding are being acquired in the microscope, the emulsion production device is connected to the syringes with the aqueous and oil phase to start of the emulsion production. By varying the flow rates of both fluids, it was possible to create different sizes of droplets with 3 distinct sizes used in the experiments.

After all the volume of desired emulsion is created, the pump injecting the oil into the emulsion creation device is stopped and the water flow rate is reduced to the same flow rate used during the water flooding previously performed. After waiting a time for the stabilization of the flow rate in the system, and to ensure that the exit tubing is completely saturated with emulsion and no air is left in it, the exit tubing of the emulsion production device is connected with the entrance of the porous media device. For a better mobility of the drops, as due to their density they have the tendency to move upwards during the flow, the porous media device is kept vertically above the emulsion production device during the emulsion flooding.

The emulsion flooding is then sustained until all the drops enter the micromodel. Afterwards, a supplementary water flooding is conducted until the

volume injected in this second step of the experiment, that is the emulsion flooding and the supplementary water flooding, is the same as the one injected during the initial water flooding. After that volume is reached the injection of water is ceased and the entrance and exit of the micromodel are closed.

With the end of the flooding process, the micromodel is again taken to the microscope for another phase distribution evaluation and image acquisition, Figure 28 shows a section of the micromodel after the emulsion flooding. Afterwards the process of cleansing of the porous media device is started.

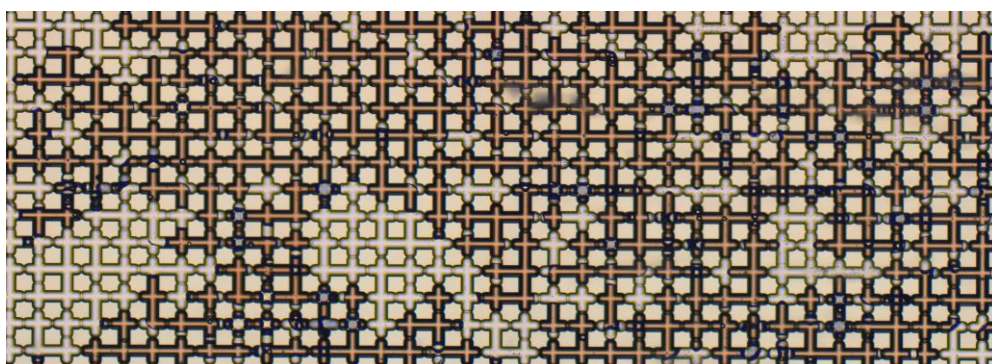


Figure 28-Sections A13 and A14 of the micromodel after the emulsion flooding of the 175 μ m drops. Aqueous phase colored with a red dye, droplets colored with a black dye and oil transparent.

The 42 images of the micromodel, taken after each step of the experiment, are then united in their correct positions forming one picture showing the effects of the experiment in the phase distribution in the entire porous media device. This image is then treated with the ImageJ software, allowing us to better differentiate the colors of each phase and to get to a minimum the borders of the porous media channels and to remove as best possible any interference or shadow that may exist in it.

After the treatment, the image of the micromodel is ran through a macro in the imageJ program that helps differentiate the phases in the image. The macro with the water being colored white and the oil black, allowing for a better visualization of each phase, as shown in Figure 29.

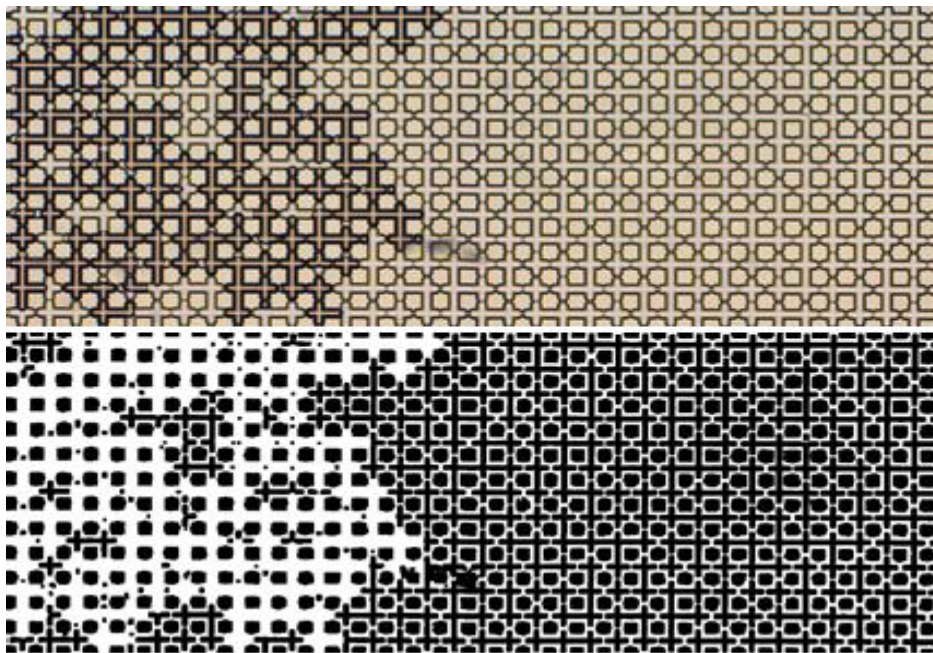


Figure 29- Sections A13 and A14 after a water flooding after and before the macro. Up before the macro with the water as red and the oil as transparent, beneath after the macro with the water white and the oil black.

The program, through the usage of the measure command, allows us to evaluate the image and calculate how much of its area colored black, in percentage is. It is important to evaluate that the areas in the image that are colored black after the treatment are the channels still saturated with oil and the solid glass between the channels, so it was necessary to evaluate the volume of the solid matrix, which were found to represents 33.3% of the porous media device area. So with that, after calculating the area in the images that effectively acts as the porous media by subtracting the solid matrix, it allows for the identification of the volume of residual oil after the water and emulsion flooding.

With the knowledge of the residual oil saturation after the water flooding and after the emulsion flooding we can calculate the volume of oil that was mobilized by the injection of the emulsion in the porous media, by subtracting this two values. The gain that the emulsion flooding resulted in can also be evaluated, by reducing the difference between the water and emulsion flooding of the 4% of pore volume in oil that was injected in the porous media in the form of droplets.

Utilizing the images of the micromodel after the emulsion flooding it is also possible to analyze the distribution of the drops along the porous media. Even with the black dye, the program has some difficulty to separate the drops from the other phases, as it would require grouping the water and the original oil in place together, so it became necessary to manually count the drops in each area of the model.

For the evaluation of the drop distribution inside the porous media, the images of the micromodel after the emulsion flooding are organized in their vertical sections, resulting in 14 images. The number of drops in each of this this sections are then counted and compared between each other and with the number of drops that we expected to have injected into the micromodel, this total number can be calculated by comparing the volume of each drop with the total volume of oil injected during the emulsion creation.

3

Results and Discussions

In this section we will be presenting and discussing the results of the experiments of water and emulsion flooding in a porous media device. For a better understanding of the effect of the size of the droplets injected and as well to better be able to compare the other aspects of the experiments the results will be grouped by the capillary number of the experiment.

For a better comprehension of the results of the experiments it was also analyzed the drop distribution and drop size distribution inside the porous media at the end of the experiments. For the acquisition of such data a vertical section of the micromodel was evaluated with the microscope software allowing us to measure the diameters of the drops in each image and with that calculate an average diameter in each section of the porous media. With this information we can understand if the drops are suffering any deformation or are breaking while flowing through the pores.

Similarly, with the same software we are able to mark and count the exact number of drops present in each vertical section of the porous media. Knowing the number of droplets in each area we can understand the behavior of the emulsion as well as understand their blockage pattern and in which areas they are more and less concentrated.

For each different scenario contemplated during the experiments, meaning for all distinct combinations of capillary number and drop size, two experiments were conducted in different micromodels in order to compare the results and analyze if they were coherent in similar situations. As exemplified by the error margin in the results presented in this section, the results were similar for the situations demonstrating a certain level of repeatability in the experiments and leading to the belief that no further repetition was necessary.

3.1

Emulsion Production

At the beginning of the experiments a few key decisions were necessary to be taken regarding the emulsions and their formation process in order to optimize the experiments and for them to provide clear results. Most of these decisions were taken based in the bibliography and the available literature about the emulsion formation through low energy methods or through experimental trial and error.

Initially it became necessary to decide on a parameter for the control of the volume of created emulsion. It was fundamental to be consistent in this injected volume or it would not be possible for an evaluation of the effects of the parameters that we were changing, and wanting to appraise, if the volume wasn't homogenous in all experiments or it wouldn't be possible to differentiate its effects from the others.

After an evaluation of the possible control parameters, it was ultimately decided to standardize the volume of oil used during the emulsion creation, meaning that we controlled the volume of created emulsion through the volume of its dispersed phase. This was the decided as it could be easily controlled, as the pumps utilized during the experiments were able to be programed to stop the injection after a certain volume or time. Controlling the volume of injected oil for the emulsion creation also allowed for a better comparison between the volumes of oil recovered with the emulsion flooding and the volume injected in the form of drops, with that granting us the possibility of calculating the effective oil gain with the emulsion flooding and thorough it assessing the economic viability of the procedure.

With the parameter standardized, it then became necessary to decide on the volume of oil that was to be used as the dispersed phase during each emulsion flooding. Different volumes of emulsion creation were initially tested before the decision of using 4% of the pore volume of the porous media, that being 1.52 μL , as the volume of the dispersed phase during the emulsion formation. This was chosen because after revisiting the bibliography 4% was the lower volume of emulsion injected found, and initial tests presented that at higher volumes of droplets that the oil recovery was not significantly enhanced and it was of our preference to keep a low volume of emulsion

injected in order to better visualize the effect of each drop and to keep the financial viability of this procedure more likely.

Another challenge discovered with the initiation of the experimental phase was the necessity of coordinating the oil and the aqueous phase to reach the T-junction in the formation micromodel at the same time. This necessity arose from the first experiments where after initiating the injection of both phases in the micromodel the water constantly reached the junction first, as its flow rate used for the emulsion formation was considerably higher than the oil, started forming a dispersed phase of air in the water until the oil also reached the junction. This unwanted emulsion was problematic as it affected the results of the experiments.

Initially we tried to bypass this problem by starting the injection of the oil first and only starting the water injection after it had reached the junction. Nevertheless, this resulted in a thin film of oil wetting the constriction, which led to the droplets being formed outside the constriction, and subsequently, without the proper size. Therefore, the solution found was using a longer tubing for the water and starting the oil first and once it was close to the junction starting the water in order for the two fluids to reach the constriction at approximately the same time.

3.2

Low Capillary Number

The experiments performed at the lower capillary number were conducted with all flooding fluids being injected at a constant flow rate of 0.065ml/h, resulting in a capillary number of 3.5×10^{-7} . This flow rate was stipulated based on a capillary study previously realized by Avendaño et al. [40], which demonstrated that performing the initial water flooding at this flow resulted in a sufficient residual oil saturation for any possible effect arising from the droplets injection in the system to be noticed. Although the residual oil saturation with this capillary number still differs from the one found in the literature in water flooding in reservoirs, being considerably lower, due to

the nature of the experiment and the size of the porous media being utilized, the goal in the present analysis is to evaluate the changes related to the emulsion injection step.

All the experiments at this lower capillary number, independent on the size of the injected emulsion did not present any droplets exiting the porous media device. This information is critical when taken in consideration that the presence of drops inside the porous media at the ending of the flooding represents the possibility of a pore being effectively blocked, and with all the produced drops still inside the micromodel at the end of the experiments could mean an efficient emulsion flooding.

3.2.1

Residual Oil Saturation

The residual oil saturation for the experiments performed at low capillary number are shown in Table 4.

| Drop Size(μm) | S_{or_w} (%) | $S_{or_{WAE}}$ (%) | Net Gain (%) |
|----------------------------|------------------|--------------------|--------------|
| 80 | 50.09 ± 1.33 | 23.96 ± 1.17 | 22.13 |
| 120 | 49.92 ± 0.9 | 21.17 ± 0.52 | 24.75 |
| 175 | 50.23 ± 1.15 | 32.47 ± 0.92 | 13.76 |

Table 4- Residual oil saturation after water flooding and emulsion flooding for the different sizes of emulsion drops.

As demonstrated in Table 4, for the experiments conducted with this capillary number, the emulsion flooding had a positive effect in the oil recovery will all used droplet sizes, although the residual oil saturation varied with the size of the emulsion drops. Experiments at this flow rate presented a positive gain in the volume of recovered oil, meaning that the volume of oil that the emulsion flooding was able to further mobilize was superior to the volume of oil injected in the porous media in the form of the dispersed phase of said emulsions. When considering the additional oil recovery due to the emulsion flooding it must be noticed that it can occur because of

two beneficial effects that the flooding can have in the oil recovery, one in a macroscale and the other in a microscale.

The macroscopic effect resulting from the emulsion flooding is that as the droplets flow with the continuous water phase through the porous media, they may cause a blockage of the pores in the preferential paths created during the initial water flooding. With the preferential paths blocked there is a reduction in the water mobility and a flow diversion occurs, forcing the water to go through different sections of the porous media that had previously been unscathed resulting in a better sweep efficiency with the mobilization and recovery of the oil in those areas.

Microscopically the resulting effect of the droplet injection derives from the increase in pressure associated with them. As previously stated, the dispersed phase of the emulsion can be responsible for a blockage of some pores along the porous media during the flow and with these blockages results in an increase in the pressure around the affected area. When this blockage occurs in an area around some oil ganglia the pressure increase may be enough to surpass the capillary pressure along the length of the ganglia, and with that, result in mobilization of said ganglia.

3.2.2

Emulsions Size Analysis

Comparing the results for each condition, we will have a better understanding of how the size of the dispersed phase of the emulsion in comparison to the size of the pores affects the efficiency of the emulsion flooding.

During the experiments it was used emulsions with droplets sizes of 80, 120 and 175 μm , with those sizes being decided due to the different sizes of the constrictions present in the porous media. These sizes resulted from the intent of having on size of drops larger than the channel, one drop approximately the size of the main channels and one between the two sizes of constrictions present as the pores. When considering the sizes of the emulsions to be used in the experiments, it was important to take into consideration that the oil drops do not act as a solid particle acting more as

a soft material, suffering deformation due to the pressure and constriction. Because of this behavior, it was possible to utilize in the experiments emulsions whose dispersed phase was composed by oil droplets that were larger than the channel of the porous media, as the drops would be able to deform.

3.2.2.1

Large Emulsions

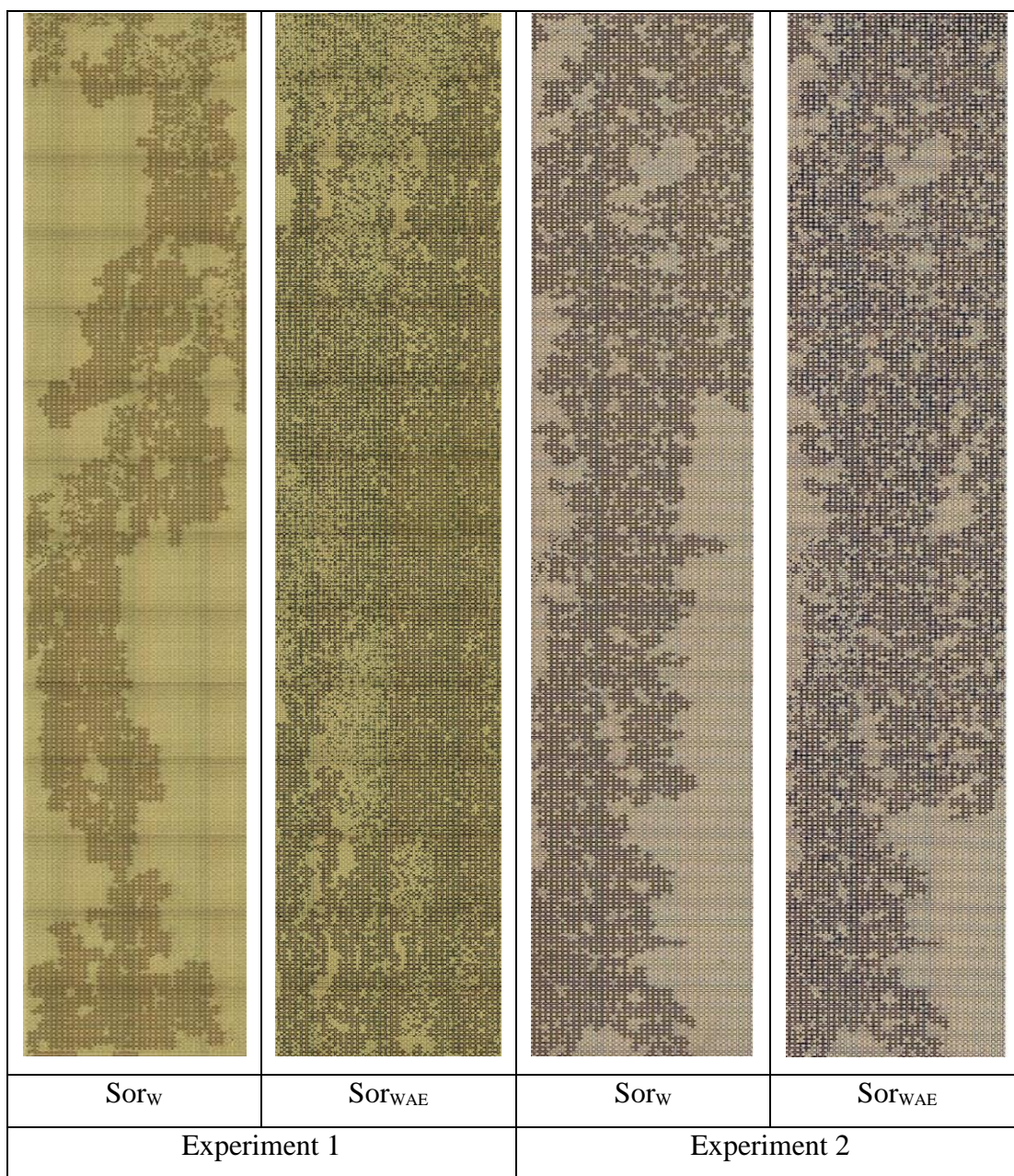


Figure 30 Images of the micromodel after the water flooding and emulsion flooding of the experiments performed at a $Ca=3.5 \times 10^{-7}$ and with dispersed phase of the emulsions with a size of $175 \mu m$. Flow from top to bottom

Figure 30 shows the phase distribution in the micromodel after the different steps in the experiments performed with the emulsions of $175 \mu m$ and the capillary

number of 3.5×10^{-7} . In all the images the flow direction occurs from top to bottom and the white phase is oil while the dark phase is water.

An observation of the phase distribution in the experiments indicates large oil ganglia still in the porous media after the end of the experiment, with in some experimental scenarios demonstrating little to no variation in the size and volume of some oil ganglia. This indicates that although beneficial to the oil recovery of the porous media as a whole, the emulsion flooding performed with these characteristics is not locally beneficial in the entire porous media, resulting in zones where the oil ganglia did not felt the effects of the emulsion being injected.

When analyzing the images of the experiments performed with the larger emulsions it was clear that, as the dispersed phase was larger than the channel of the porous media the drops were constantly being compressed. The pore blockage occurred with a single drop occupying the entire pore section. Due to their size there were also situations where the droplets were blocking the channels of the micromodel in some areas, differing from the experiments conducted with the other drop sizes whose blockage occurred only in the pores of the porous media.

Although the usage of the emulsions of $175 \mu\text{m}$ proved to be beneficial to the oil recovery resulting in the mobilization of a larger volume of oil than that injected in the dispersed phase of the emulsion, it was the least effective of the emulsions tested during the experiments at this flow rate. This result can possibly be explained by the fact that the emulsion size was too large in comparison to the pores which resulted in a less effective blockage due to the constant deformation that the drops were subjected to during the flow.

It is important to notice though that as we are controlling the volume of emulsion created through the volume of the dispersed phase and keeping it constant for all scenarios the experiments conducted with the larger drops were also the ones with the lowest quantity of injected drops in the porous media.

When analyzing the size distribution of the drops of this size at the end of the experiment it was not possible to analyze the diameter of the drops due to its size being

larger than that of the channel of the porous media, the drops were constantly being deformed and compressed resulting in a dispersed phase that more often than not did not present itself in a spherical form. Figure 31 exemplifies one section of the micromodel with the larger drops size being analyzed displaying the deformation in some of the droplets.

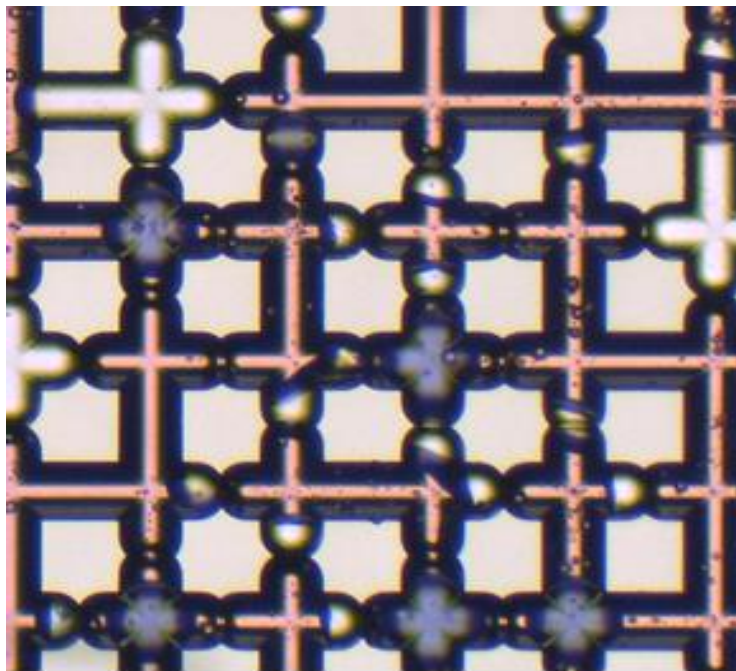


Figure 31- Section of the porous media after emulsion flooding with large drops exemplifying their deformation.

Besides the drop deformation, in this image of the porous media it is also clear that some of the droplets are considerably smaller than the original produced size, with this difference made clear by the comparison with the deformed drops. This illustrates the possibility of breaking of the droplets, especially the larger ones, as they flow through the constrictions in the porous media.

3.2.2.1.1

Drop Distribution in the Porous Media

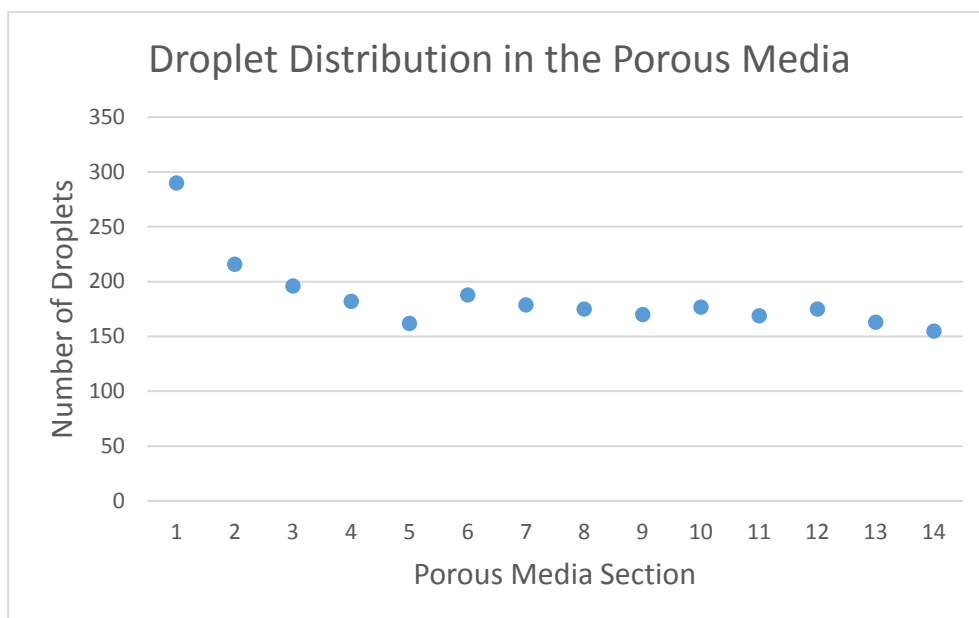


Figure 32- Drop distribution along the porous media in experiment performed with droplets of $175\mu\text{m}$

Figure 32 shows the distribution of the number of drops in each vertical section along the micromodel. This curve demonstrates a tendency of the drops to be concentrated in the pores of the micromodel closer to the entrance of the porous media.

After the bulk of the produced droplets are clogging the initial pores their concentration along the rest of the porous media remain similar. This difference in the concentration of the drops along the length of the micromodel is likely due to the size of the dispersed phase of the emulsions, as they are larger than the channel of the porous media, resulting in most of the droplets presenting difficulty to flow through the pores with the biggest constrictions and blocking those initial pores. With most of the drops blocking the initial pores, the volume of free droplets traveling the micromodel is severely reduced representing one explanation for the lower number in the rest of the porous media. It is also of importance to understand that as the drops flow through the pores they may suffer deformations or break resulting in droplets with an effective

diameter different than the one initially produced, and for this reason their blockage efficiency and capacity may be reduced.

This tendency in the blockage of pores is important when analyzing the oil recovery in the porous media. With the concentration of pore blockage occurring in the entrance of the porous media the oil ganglia closer to the exit of the micromodel end up being less affected by a local pressure increase resulted from the pore blockage, with its mobilization being affected primarily by the alteration of preferential paths. This diminished pressure effect due to the reduction in the number of drops along the porous media, resulting in a loss of one of the mobilization methods for the oil ganglia in the ending sections of the micromodel, may help explain the reason for the experiments conducted with the larger emulsion presenting the less volume of recovered oil. These experiments presented a large decrease in the number of emulsions along the porous media, with a reduction in the number of droplets between the entrance and the exit of the micromodel being of 47.6%.

3.2.2.1.2

Size Distribution

Due to the size of the particles in comparison to the channel of the porous media, resulting in the droplets being in a constant state of deformation during the flow, the drops did not present a spherical form at the end of the experiment. As the drops were no longer spherical, it became impossible to gauge its diameter and subsequently its size.

Although a precise size of the drops could not be obtained, it was possible to visually analyze them at the end of the experiment and it became clear that there were different sizes, indicating that during the flow some of the droplets were breaking as they passed through the pores. Figure 33 demonstrates the difference in size and aspect in the drops near the entrance and the exit of the porous media.

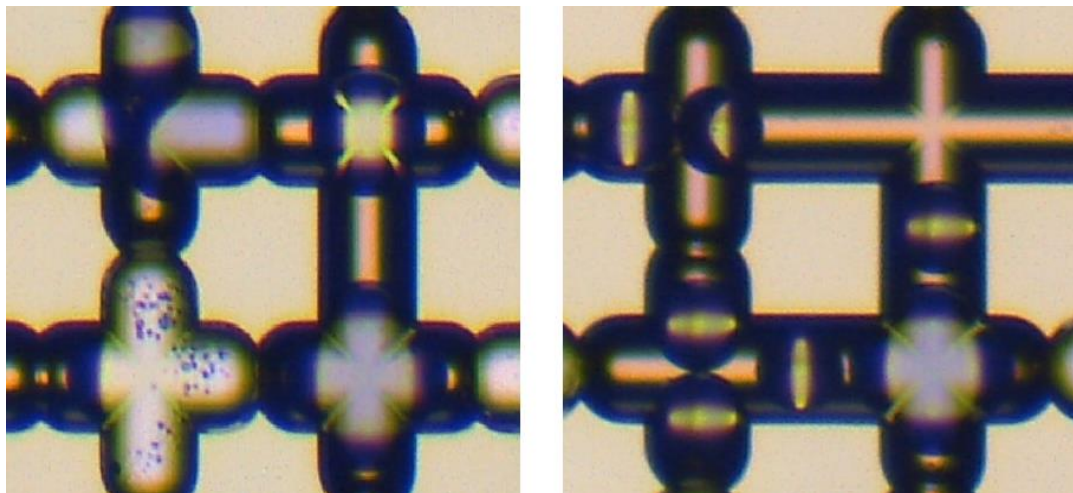


Figure 33- Difference in the drops in the entrance and the exit of the porous media, left and right respectively.

With this observation, it was possible to conclude that although the drops are soft and capable of being deformed, the effects of the flow through pores considerably smaller than them led to breaking of the disperse phase, which is clear in Figure 33 (right). This is important as it leads to a polydisperse flooding, with the droplets breaking in different sizes and suffering individual effects.

3.2.2.2

Medium Emulsions

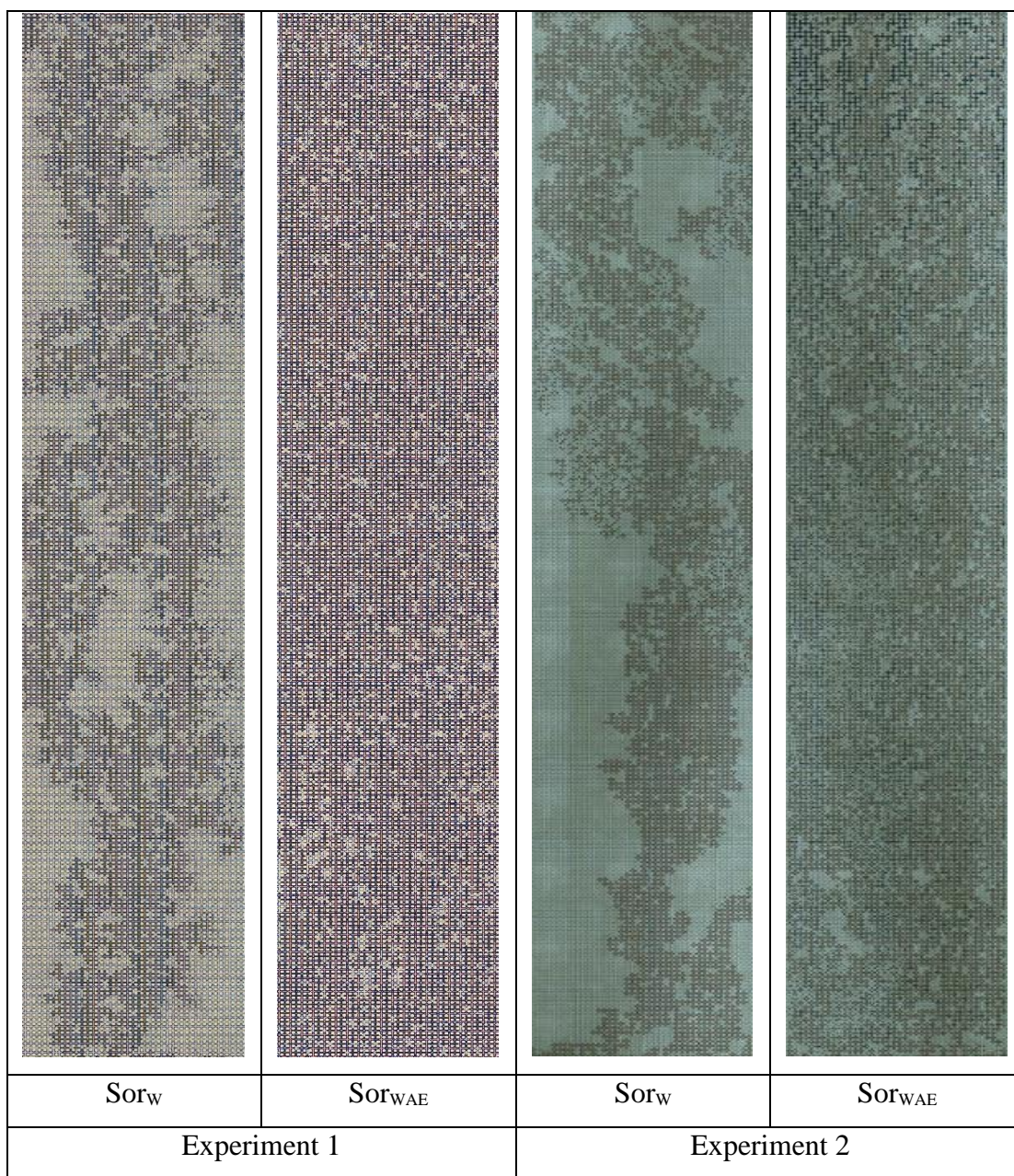


Figure 34- Images of the micromodel after the water flooding and emulsion flooding of the experiments performed at a $Ca=3.5 \times 10^{-7}$ and with dispersed phase of the emulsions with a size of $120 \mu m$. Flow from top to bottom

Figure 34 shows the phase distribution in the micromodel after the different steps in the experiments performed with the emulsions of $120 \mu m$ and capillary number

of 3.5×10^{-7} . In all the images, the flow direction occurs from top to bottom and the white phase is oil while the red phase is water.

An analysis of the phase distribution in the experiments performed with the drops of $120\mu\text{m}$ demonstrates that all the large oil ganglia that were left in the porous media after the initial water flooding were affected by the emulsion injection, with most the oil that was left in the micromodel at the end of the experiment being composed by small ganglia. This effect in the large ganglia is important as their mobilization in all the areas of the porous media indicates that both the alteration of the water paths as well as the increase in localized pressure are occurring effectively and having a positive effect.

The injection of the emulsion of $120\mu\text{m}$ at this lower flow rate demonstrated a positive effect in the oil recovery of the porous media, resulting in a mobilization of a significant amount of the volume left after the initial water flooding. The volume of oil recovered with this process indicates that the emulsion injected was capable of performing an effective block in the pores of the micromodel resulting in the diversion of the water and increase in local pressure, two mechanisms expected for the recovery of the small and larger oil ganglia through the porous media.

Being close to the size of the channel of the porous media the drops of $120\mu\text{m}$ only demonstrated effects of deformation due to compression when flowing through the pores and constrictions of the porous media, resulting in droplets that mostly did not lost their original spherical form. Due to the similarity in size between the injected drops and the channel of the porous media, the blockage more commonly were performed by a single droplet in each pore, resulting in a well spread distribution of the disperse phase during the flow.

3.2.2.2.1

Drop Distribution in the Porous Media

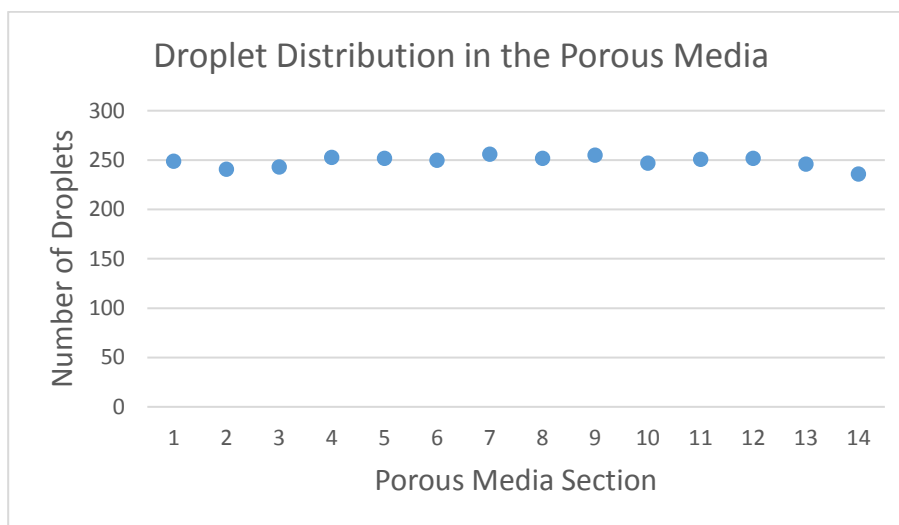


Figure 35- Drop distribution along the porous media in experiment performed with droplets of $120\mu\text{m}$

Figure 35 shows the distribution of the number of drops in each vertical section along the micromodel. An observation of the curve indicates that this emulsion flooding process resulted in droplets well spread across the porous media with similar concentrations in all sections.

The injection of emulsion with a disperse phase of $120\mu\text{m}$ resulted in an even spread of droplets along the porous media. The droplets are well distributed through the length of the micromodel due to their size being proportional to the size of the channel, resulting in a more easily flow through the porous media by the dispersed phase, allowing for drops to better pass through the initial pores and affect the later sections of the micromodel. The experiments with this drop size resulted in the lower reduction in the number of drops along the flow, with a reduction of 5.3% from the entrance to the exit.

This equal distribution of the drops along the length of the micromodel is important to help understand the oil recover of the experiments conducted in these conditions. With a better distribution of the dispersed phase of the injected emulsion, the water creates more paths to flow through as the drops blocks the old ones, leading

to more areas of the porous media being susceptible to the effects of the flooding resulting in oil ganglia in different parts of the micromodel being mobilized.

3.2.2.2.2

Size Distribution

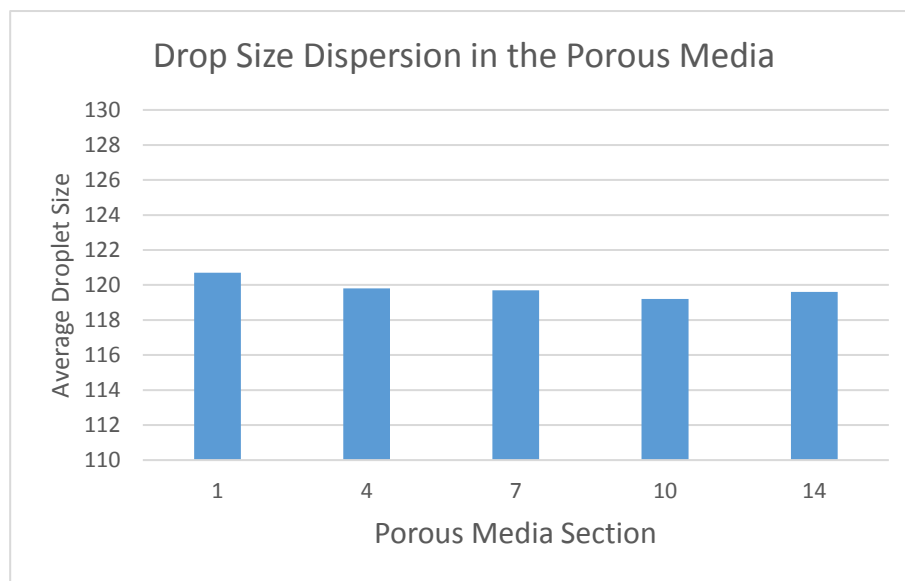


Figure 36- Droplet size distribution along the micromodel for injection of drops of $120\mu\text{m}$ with a $Ca = 3.5 \times 10^{-7}$.

Figure 36 shows the average drop size of the emulsions disperse phase along the porous media after the emulsion flooding. The presented curve demonstrates that the droplets of $120\mu\text{m}$ do not suffer any significant alteration in their average drop size as they flow through the porous media.

With the disperse phase maintaining on average their original size during the flow it results in an important level of monodispersity during the emulsion flooding process, which guarantees a more similar blockage in all areas. This similar drop size is important for a better comprehension of the effects of the injection of a drop of the same size of the channel of the porous media, where if the drop size had been highly affected by the injection, such as the larger drops were, a conclusive inference on the effects of the injection of this particle size would not be possible.

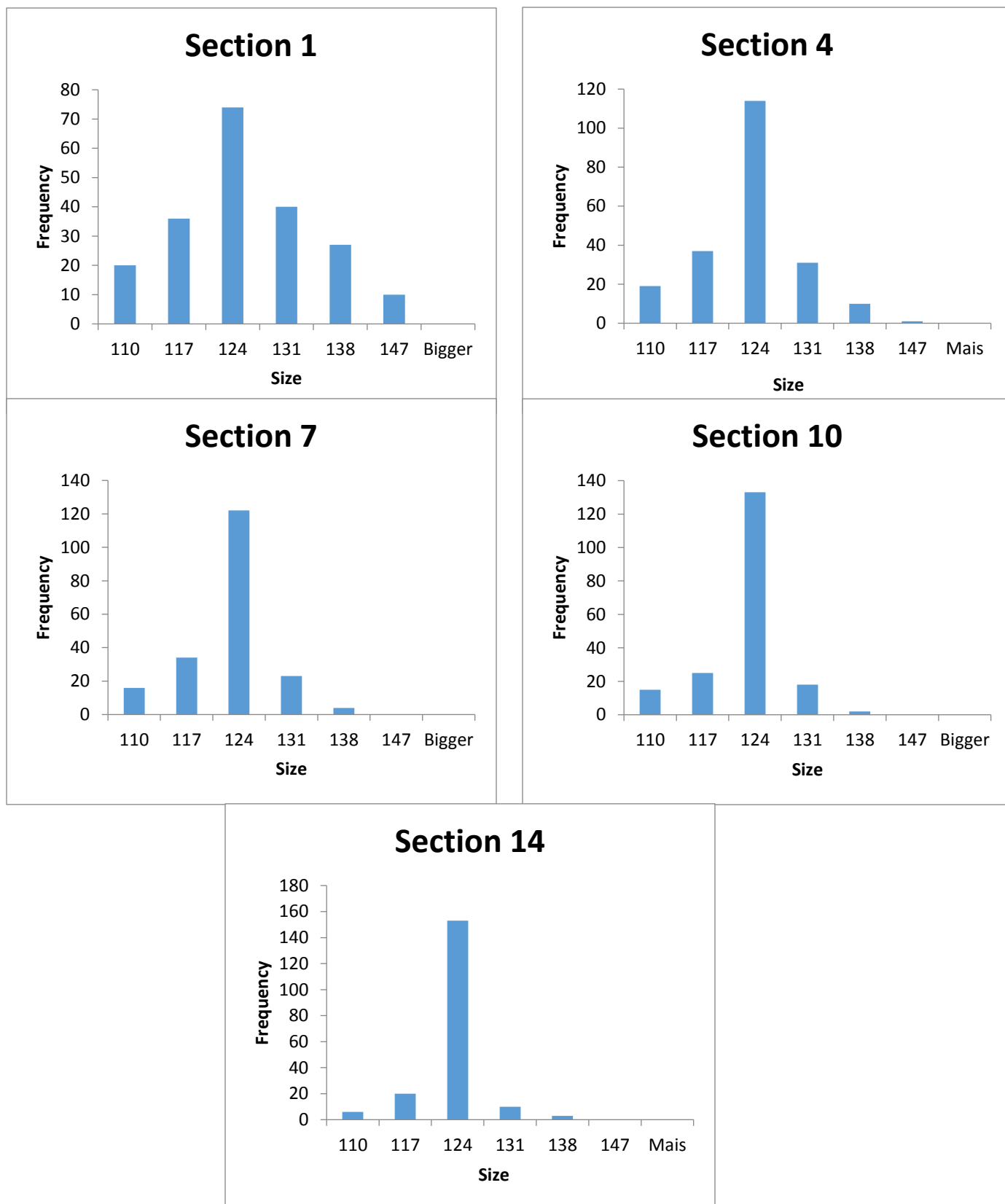


Figure 37- Drop Size distribution of the porous media at 0.065ml/h and a dispersed phase of 120 μ m.

Figure 37 present the particle size distribution in section 1, 4, 7, 10 and 14 of the porous media after the emulsion flooding performed with the lower flow rate.

Observing the histograms of size distribution in each section of the porous media, it demonstrates that although the average drop size does not suffer significant alteration during the flow through the porous media in each section the concentration of drops of different sizes differ, but still with a higher concentration of the produced size in all sections.

In the entrance of the micromodel there is are a bigger presence of the droplets of different sizes, with a tendency of a reduction in the number of these as the flow occurs. The drops suffer effects from the entrance of the porous media, resulting in the bigger concentration of distinct sizes in the first section, but as they flow through their softness allows for small deformations for passage through pores, leading to a decrease in the number of coalescence and breaking of droplets and a higher concentration of the original size in the drops.

3.2.2.3

Small Emulsions

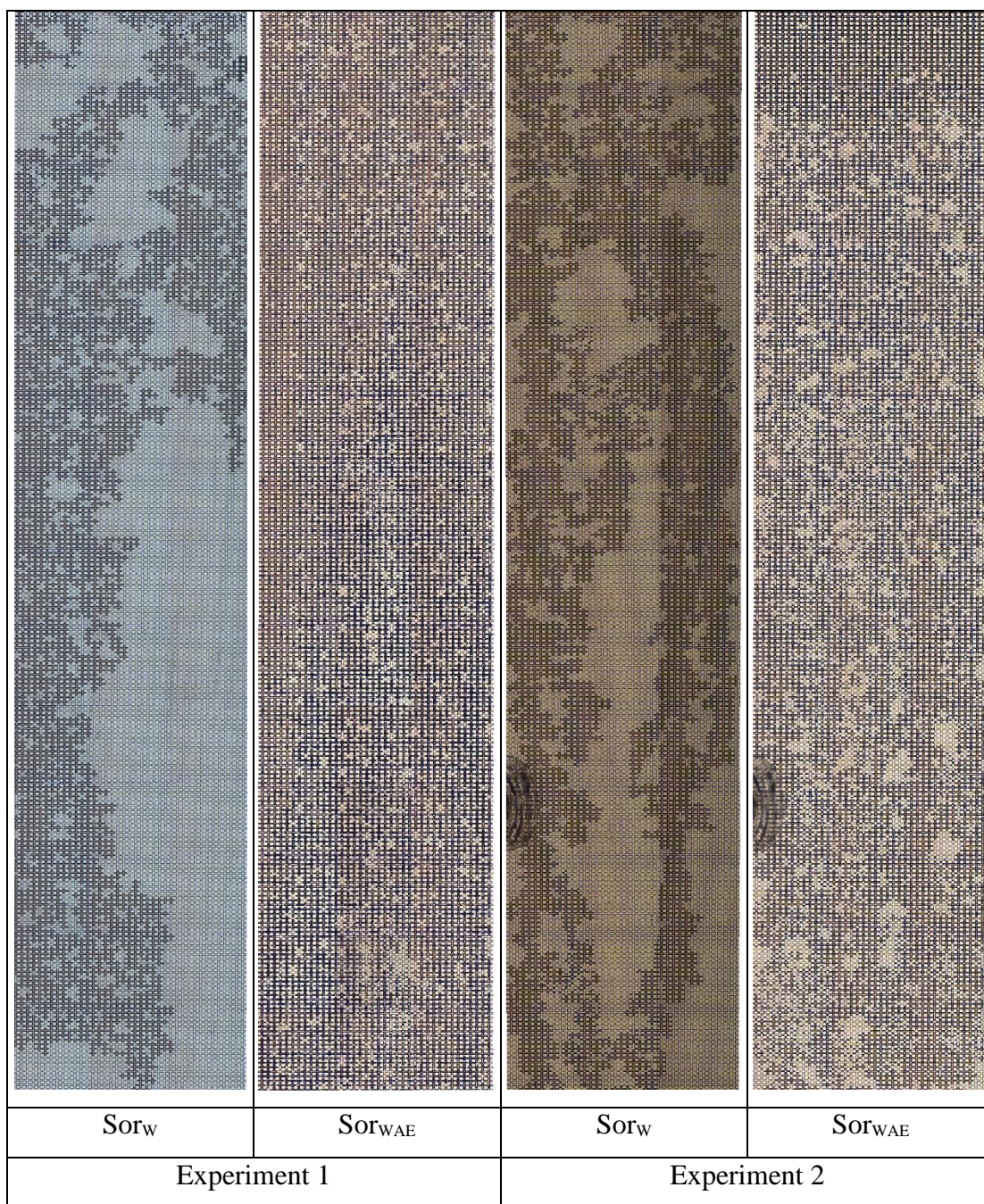


Figure 38: Images of the micromodel after the water flooding and emulsion flooding of the experiments performed at a $Ca=3.5 \times 10^{-7}$ and with dispersed phase of the emulsions with a size of $80 \mu m$. Flow from top to bottom.

Figure 38 shows the phase distribution in the micromodel after the different steps in the experiments performed with the emulsions of $80 \mu m$ and the capillary

number of 3.5×10^{-7} . In all the images, the flow direction occurs from top to bottom and the white phase is oil while the red phase is water. During the final experiments an accident happened where a small fracture at the surface of the micromodel occurred, but after analyzing that the pores inside the micromodel had not been affected and that the small – and external - affected area in the surface did not disturb greatly the macro for phase distribution evaluation, the experiments were maintained.

Observing the distribution of the phases after the conclusion of the experiments executed with the $80\mu\text{m}$ drops it is clear the significant reduction of most of the large ganglia in the porous media, with the majority of the oil left in place in the form of smaller ganglia. This effect in the large ganglia is vital for an efficient oil mobilization as it affects residual oil in all areas of the porous media, although analyzing the distribution the ganglia in the ending of the porous media seemed to be less altered than the ones in the entrance.

The injection of emulsions of $80\mu\text{m}$ at the flow rate of 0.065ml/h proved to be efficient in the recovery of the oil left in the porous media after a water flooding, mobilizing the oil and demonstrating efficiency close to that of the $120\mu\text{m}$. It is important to take under consideration when analyzing this data that as the control parameter for our emulsion production was the volume of oil dispersed as these experiments were performed with the drops of the lowest diameter, and subsequently the lowest volume, there were bigger number of drops produced and injected in the porous media in these experiments.

As the produced droplets are smaller than the channel of the porous media and due to their deformation capacity, they may flow through the constrictions, being the same size of the larger one and slightly bigger than the smaller one, the blockage during these experiments were performed by multiple drops at a time. Unlike seen in the experiments performed with the other sizes of drops, the pores in were blocked by an agglomeration of droplets, with Figure 39 showing the blockage, resulting in an effective blockage by the pore that would not be possible with a single droplet due to its size in comparison to the porous media.

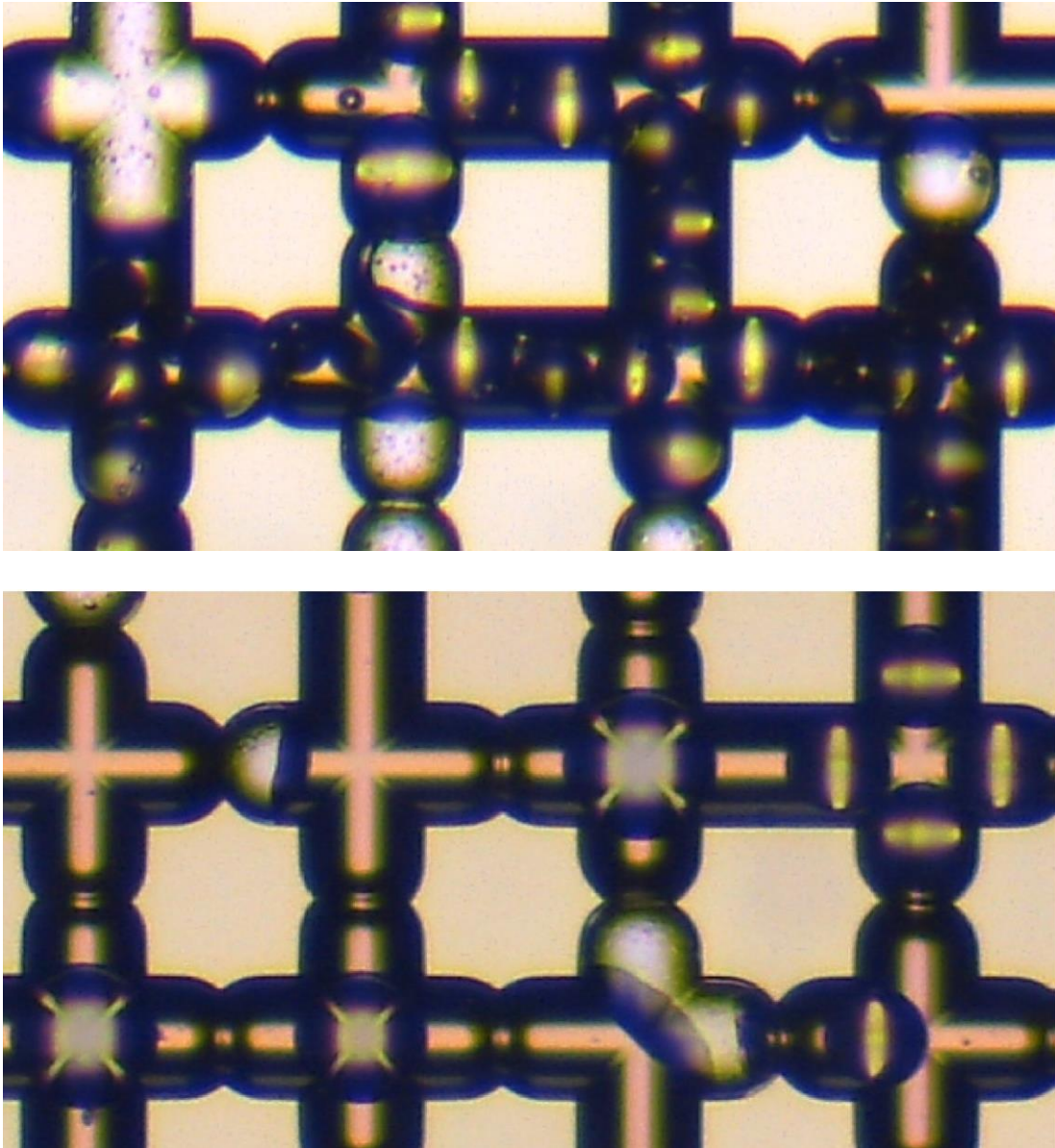


Figure 39- Pore blockage by an agglomeration of the smaller sized emulsions above comparing to the blockage by a single droplet in the flooding with the larger size below.

3.2.2.3.1

Drop Distribution in the Porous Media

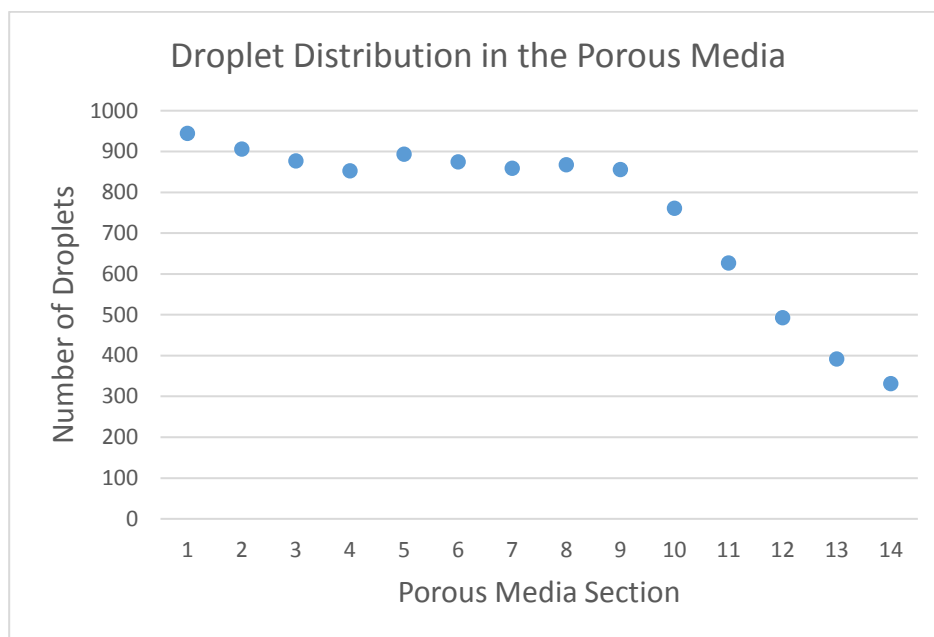


Figure 40- Drop distribution along the porous media in experiment performed with droplets of $80\mu\text{m}$.

Figure 40 shows a graphic of the distribution of the number of drops in each vertical section along the micromodel for experiment performed with the lower capillary number and the small drops. Due to the method chosen for the control of the produced emulsion these experiments presented the highest number of injected droplets, as can be seen in the plot.

Although the experiment performed with the most produced and injected droplets there is a distinct decrease in the number of droplets from the middle to the end of the porous media. This reduction in the number of drops closer to the exit of the micromodel happens due to the blockage mechanism associated with the emulsion flooding performed with this size of drops, with a group of droplets being necessary to efficiently clog a pore of the porous media. With a number of drops being responsible for the blockage of each pore, closure to the ending of the porous media the number of droplets are considerably smaller, as even with a bigger amount being injected most of it were blocking the pores in the entrance and middle portions of the micromodel. These

experiments presented the biggest reduction in the number of drops along the porous media, with a decrease of 65.8% from the entrance to the exit of the micromodel.

The similar distribution of the drops in the earlier parts of the porous media is important to explain the mobilization of the ganglia throughout the porous media, though in the ending sections of the micromodel there are more ganglia due to the decrease in the number of drops. An equal distribution demonstrates that these areas were similarly affected by the emulsion injection, and different paths for the water were created in it as well as an increase in its pressure, helping mobilize ganglia in the different sections.

3.2.2.3.2 Size Distribution

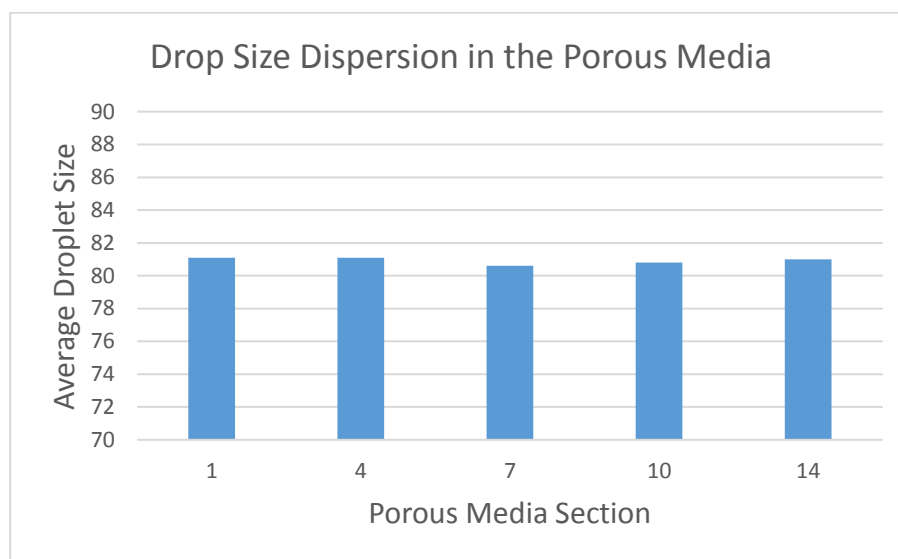


Figure 41- Droplet size distribution along the micromodel for injection of drops of $80\mu\text{m}$ with a $Ca = 3.5 \times 10^{-7}$.

Figure 41 shows a graphic presenting the average drop size of the emulsions disperse phase along the porous media after the emulsion flooding. The presented curve demonstrates that the droplets of $80\mu\text{m}$ do not suffer any significant alteration in their average drop size as they flow through the porous media being similar to the original produced size during the entire flooding.

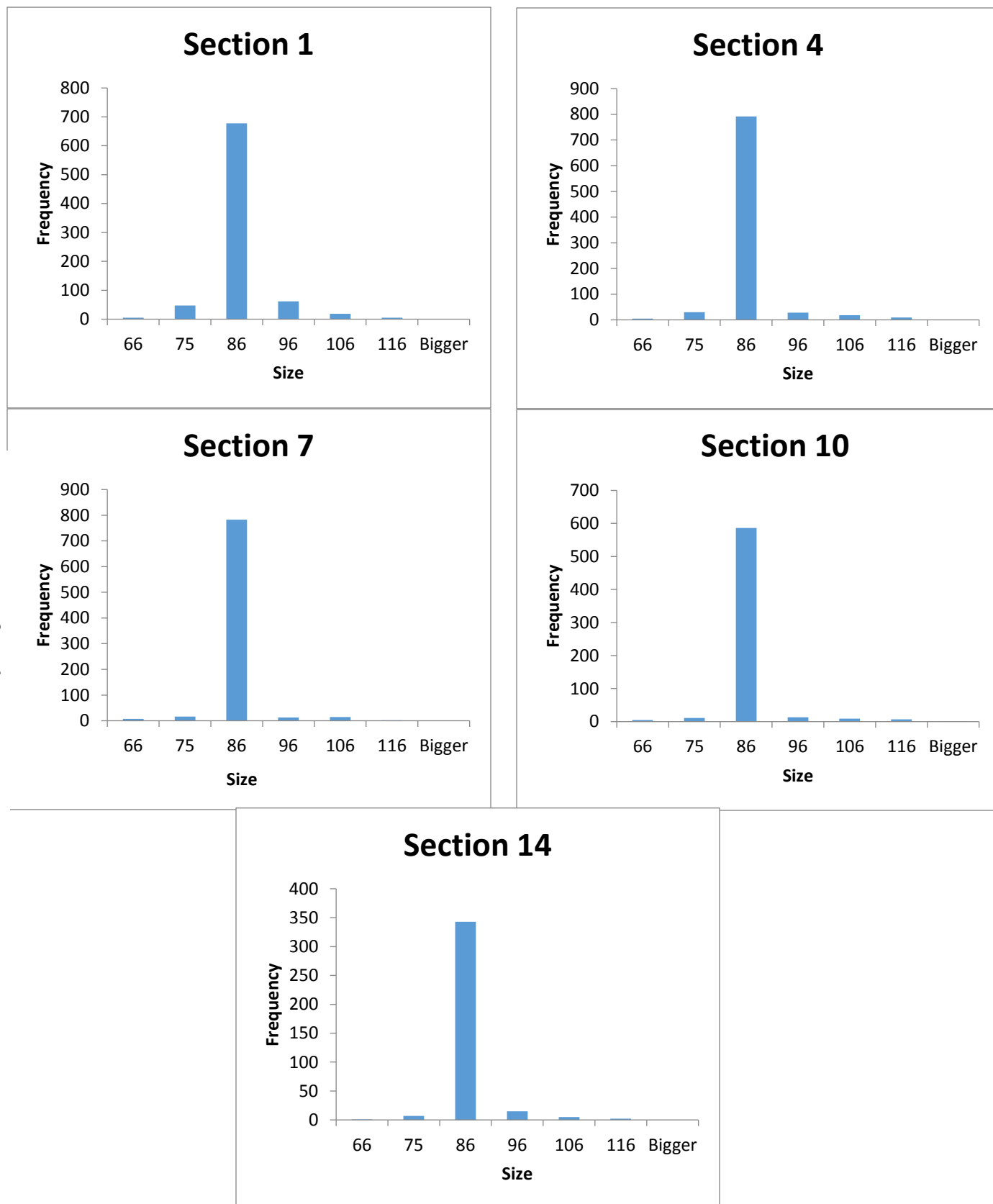


Figure 42- Drop Size distribution in the porous media at 0.065ml/h and a dispersed phase of 80 μ m.

With the size of the droplets being similar to the constrictions of the porous media they are less affected they are less subjected to strain as they flow through the porous media, resulting in being less deformed and leading to a lower occurrence of coalescence and breaking of the drops. This leads to a monodisperse emulsion injection, which leads to a similar block pattern in all areas and is important for an analysis of the behavior of the emulsion flooding.

Figure 42 present the particle size distribution in section 1, 4, 7, 10 and 14 of the porous media after the emulsion flooding performed with the lower flow rate.

Observing the local size distribution in each section of the porous media it demonstrates the small effects that the flow through the porous media has on the smaller droplets. Due to their reduced size in comparison to the channels the $80\mu\text{m}$ droplets flow more easily through the pores resulting in a small number of drops breaking or coalescing, with the vast majority keeping the original produced size.

3.3

Higher Capillary Number

The higher flow rate decision required a few tests and experimentation with candidates chosen from the literature before ultimately settling in one. Initially rates of 0.39 and 0.325 ml/h were tested as possibilities, but the results for the residual oil saturation in the porous media after the water flooding had ceased were low enough that it was close to the irreducible saturation, implying that an emulsion flooding would be meaningless in that system. Posterior tests demonstrated that an injection rate of 0.26 ml/h was high enough that it would be capable of contrasting with the lower flow rate and it would still leave enough residual oil for the experiment to be conducted. Therefore, it was decided that the flow rate 0.26 ml/h would be utilized for the experiments performed at a higher capillary number.

The experiments conducted with this capillary number, independent on the size of the injected drops, presented a significant amount of the droplets exiting the porous

media during the flow. This results in a lesser number of drops effectively blocking pores in the flow, which in turn is an indication of a less effective emulsion flooding process.

3.3.1

Residual Oil Saturation

| Drop Size(μm) | S_{orw} (%) | S_{orwAE} (%) | Gain (%) |
|----------------------------|------------------|------------------|----------|
| 80 | 21.65 ± 1.62 | 19.48 ± 0.97 | -1.8 |
| 120 | 23.73 ± 1.04 | 21.28 ± 0.48 | -1.5 |
| 175 | 22.48 ± 1.42 | 18.86 ± 0.81 | -0.6 |

Table 5- Residual oil saturation after water flooding and emulsion flooding for the different sizes of emulsion drops.

Table 5 represents the average value of saturation and the gain from the experiments performed at this capillary number using emulsion flooding with different sizes of dispersed phase.

The results from the experiments performed with the higher capillary number demonstrates a less effective emulsion flooding process resulting in a small capacity to further mobilize the oil ganglia still in the porous media. This small recovery resulted in a negative gain in the experiments with all tested droplet sizes, with a negative gain meaning that the oil injected in the porous media in the form of the dispersed phase of the emulsion was higher than the oil recovered by said emulsion injection.

The flooding process becomes less effective in this scenario because with an increase in the flow rate the droplets blockage of the pores become less effective as they deform and flow through them more easily due to the pressure increase. This effect results in reduced number of pores of the micromodel being effectively blocked by the drops, creating areas where the effects of the emulsion injection is not felt by the oil ganglia.

The negative effect in the oil recovery derive from the fact that with the increased flow pressure the drops have more difficulty in blocking a pore, as they tend to deform more and flow through. With this decrease in the number of blocked pores fewer different paths are created for the water to flow during the flooding and the build up pressure around ganglia are less efficient as sometimes during the build up the droplet stops blocking the pore and flow through the media.

When analyzing the lower recovery associated with the emulsion flooding performed with this capillary number one must remember, that the residual oil saturation after the water flooding is significantly smaller than that with the capillary number of $Ca = 3.5 \times 10^{-7}$. With the reduced volume of residual oil after the water flooding the oil left capable of mobilization at the start of the emulsion flooding is also diminished, one thing that must also be taken under consideration when considering the different factors and conditions that may negatively affect the oil recovery.

3.3.2

Drops Sizes

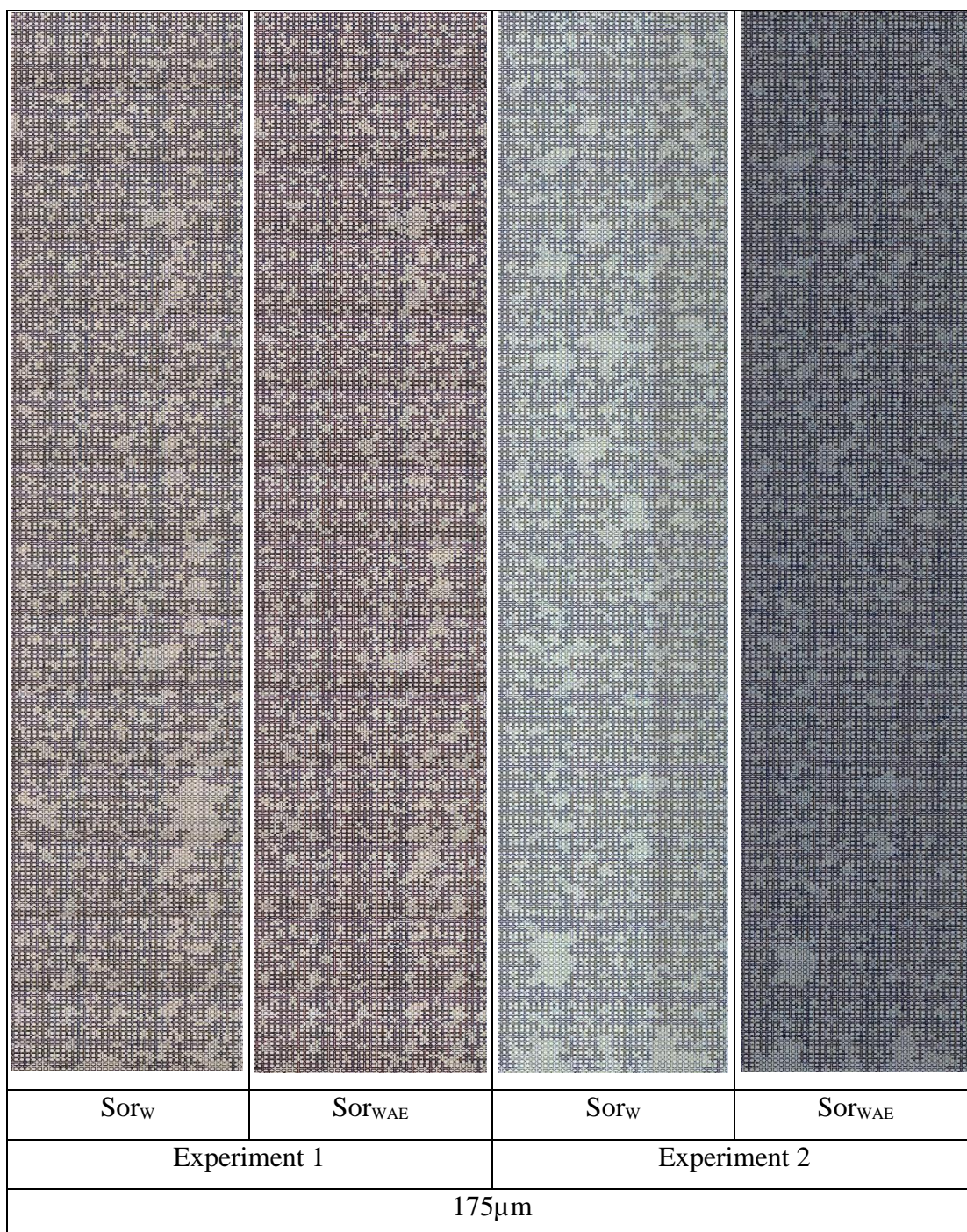


Figure 43: Images of the micromodel after the water flooding and emulsion flooding of the experiments performed at a $Ca=1.85 \times 10^{-6}$ and with dispersed phase of the emulsions with a size of $175\mu\text{m}$.

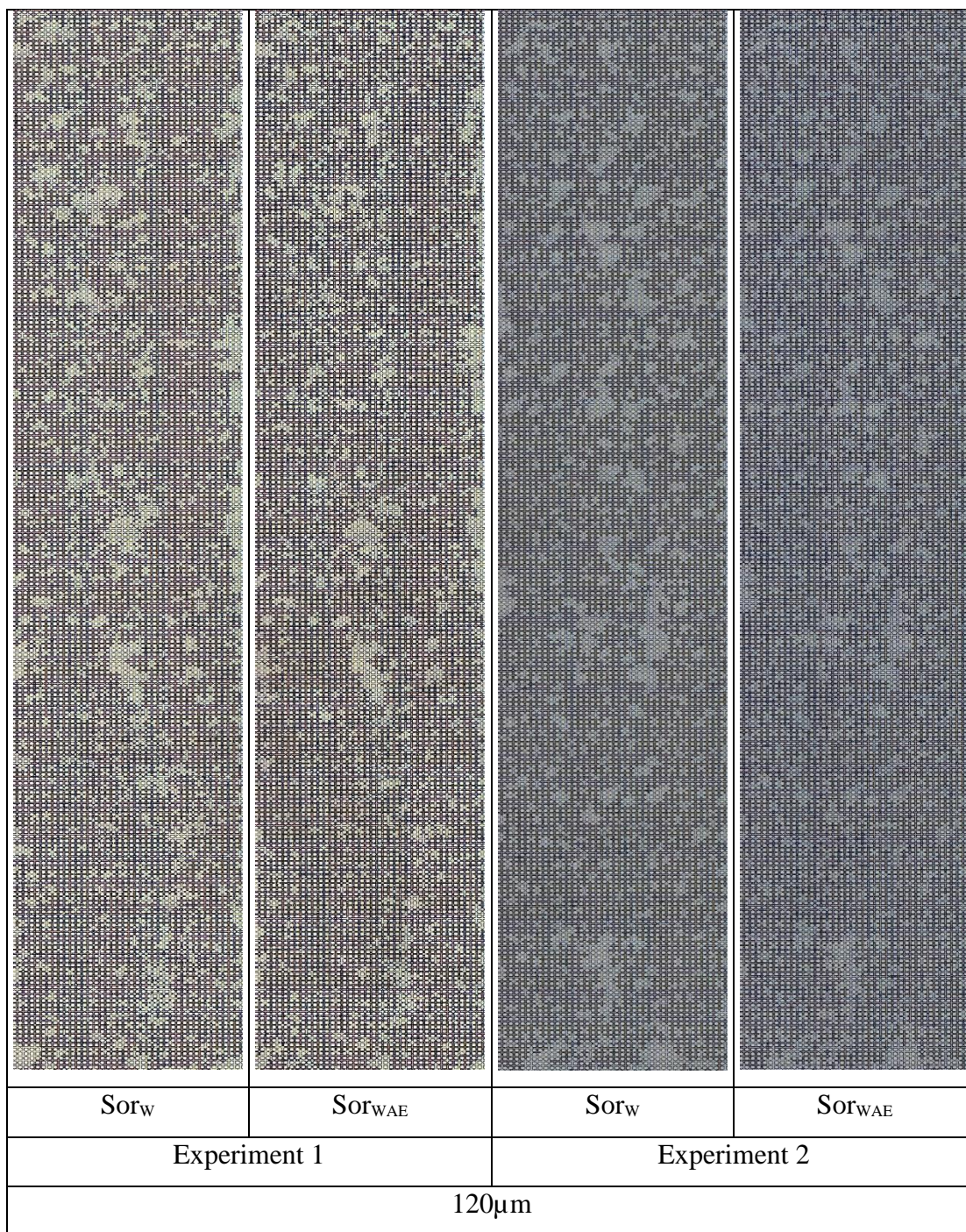


Figure 44: Images of the micromodel after the water flooding and emulsion flooding of the experiments performed at a $Ca=1.85 \times 10^{-6}$ and with dispersed phase of the emulsions with a size of $120 \mu m$.

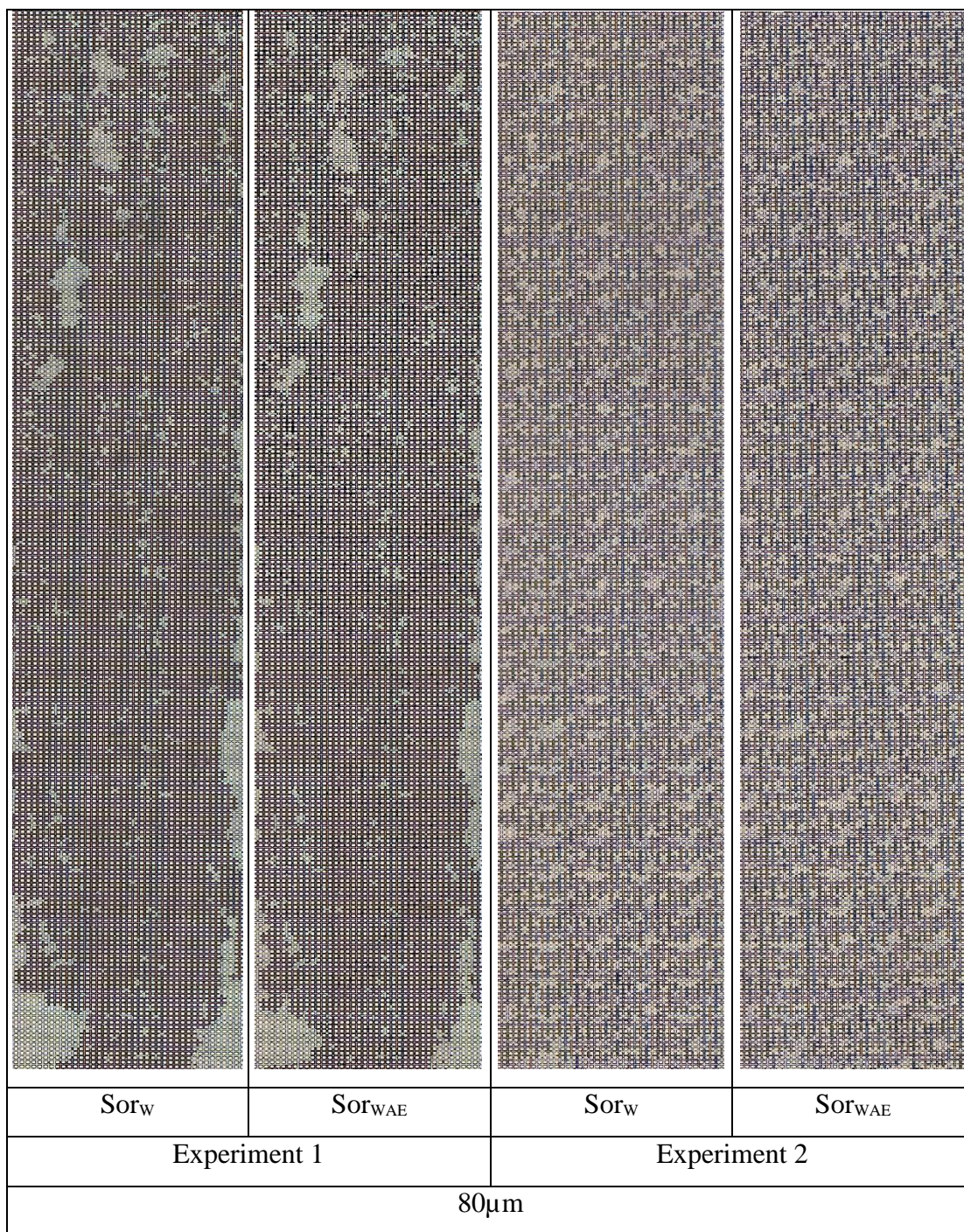


Figure 45: Images of the micromodel after the water flooding and emulsion flooding of the experiments performed at a $Ca=1.85 \times 10^{-6}$ and with dispersed phase of the emulsions with a size of $80\mu m$.

Figure 43 to Figure 45 present the phase distribution after each step of the experiments performed with the capillary number of 1.85×10^{-6} for all sizes of injected

droplets. In all the images the flow direction occurs from top to bottom and the white phase is oil while the red phase is water.

An observation of the phase distribution after the different steps of the experiments shows that the oil ganglia left in the porous media after the initial water flooding suffered little to no modification after the emulsion flooding, maintaining their initial aspect and volume. This little alteration in the oil ganglia after the emulsion flooding is an indicator that the flooding process was not as effective in the oil mobilization as it was with the lower capillary number.

Independent of the injected particle size the emulsion flooding performed with the capillary number of 1.85×10^{-6} did not present positive results as the pressure of the injection was too high for the droplets to consistently be able to block the pores of the porous media. The increased pressure, when compared to the experiments performed with capillary number of 3.5×10^{-7} , results in a larger deformation of the drops as they start to block a pore the pressure increases around the pore and possibly forcing the drops through the pore instead of blocking it.

Although still presenting a negative gain in the process, the drops of $175 \mu\text{m}$ presented the best results during the experiments, which can be explained by the fact that being considerably larger than the channel of the micromodel these drops are more capable of blocking more channels than the smaller drops would block. Similarly, the drops of $80 \mu\text{m}$ presented the worst gain, as due to their size and necessity to perform the blockage as an agglomeration, the pressure increase makes it harder for the blockage to occur, as it needs the group to stay unaffected for the blockage to be effective in the pore.

3.3.2.1

Drop Distribution in the Porous Media

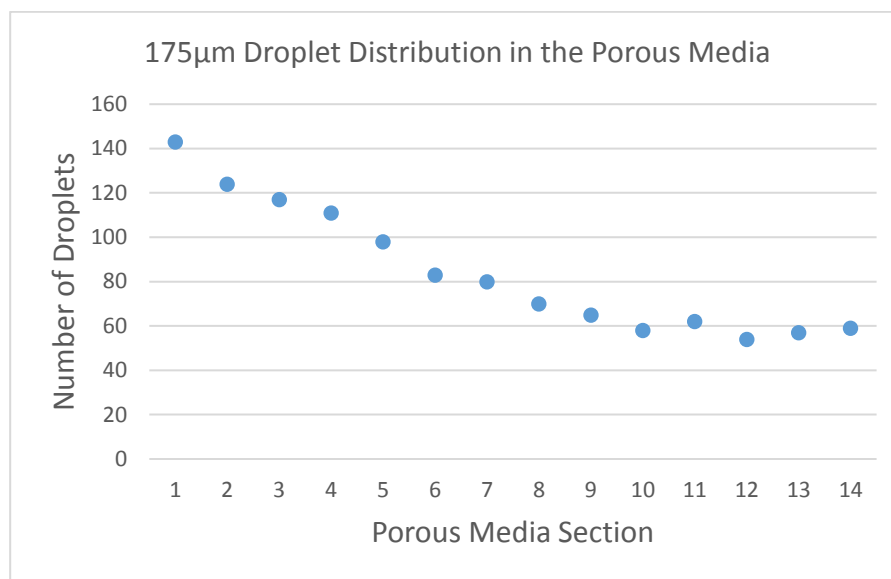


Figure 46- Drop distribution along the porous media in experiment performed with droplets of 175µm

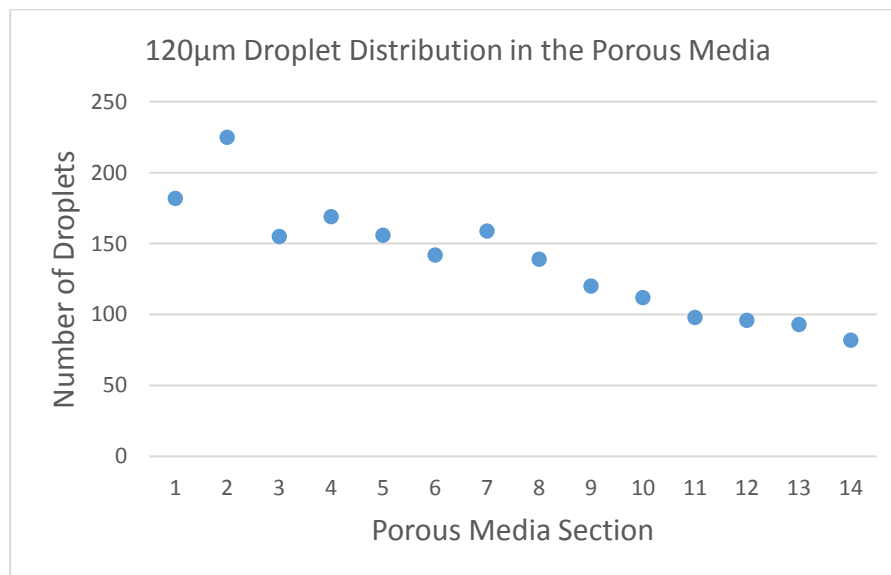


Figure 47- Drop distribution along the porous media in experiment performed with droplets of 120µm

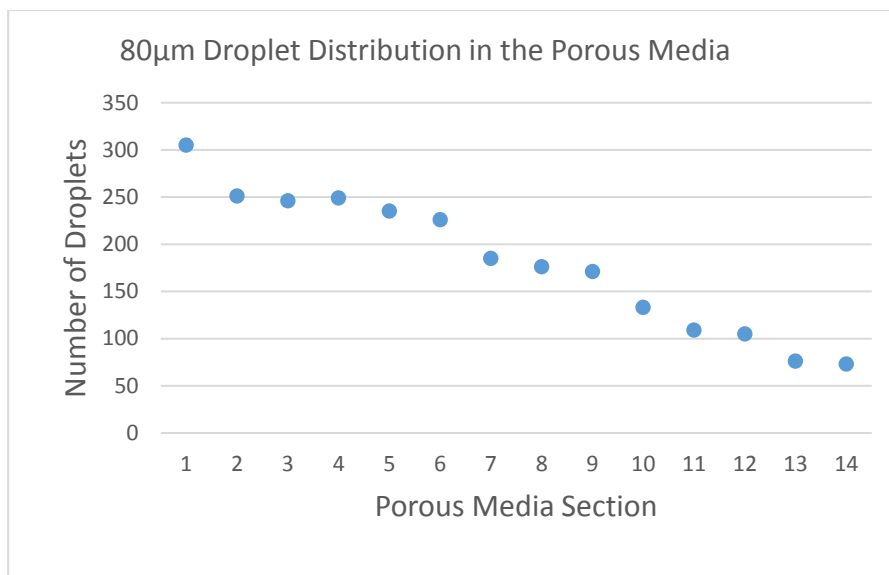


Figure 48- Drop distribution along the porous media in experiment performed with droplets of $80\mu\text{m}$

Figure 46 to Figure 48 shows the distribution of the number of drops in each vertical section along the micromodel for the experiments performed with the higher capillary number.

Observing the number of drops still in the porous media at the end of the experiments there are significantly less droplets than in the performed with the same size of drop with the lower capillary number. This reduction in the number of drops in the porous media is an indicator of what had been previously visually seen, due to the increase in the injection pressure the droplets were exiting the porous media during the emulsion flooding.

This reduction in the number of droplets in the porous media is one of the main reasons believed to cause the emulsion flooding conducted at this capillary number to be less effective. With a reduction in the number of drops in the porous media, the number of blocked pores is also reduced, reducing the positive aspects of the injection of the emulsion in the porous media.

4

Conclusion

Experiments performed demonstrated that the flow rate used during the fluid injection in the system influences heavily the effectiveness of the emulsion flooding process. The experimental results indicated that a smaller flow rate in the fluid injection results in a more efficient emulsion flooding, as it makes easier for the dispersed phase to block the pores of the porous media, as the pressure of the flow trying to force them through is smaller. Thus, an efficient WAE depends on the right moment to inject the emulsions in order to profit from the extra pressure and blockage of preferential paths.

Considering the smaller flow rate used for the experiments, the results obtained indicate the existence of an optimal drop size for the emulsion flooding process. The injection of a droplet with a size closer to the channel of the porous media presented a better recovery at lower capillary number, as one droplet was enough for an efficient blockage of the pores and they could still flow adequately to latter section of the micromodel. The drops larger than the channel presented problems in their flow capacity, resulting in most of the drops being concentrated near the entrance of the porous media which in turn leads in a weaker effect in the oil ganglia closer to the exit. In contrast, the drops smaller than the channel demonstrated an efficient blockage mechanism as well as capacity to flow through different areas of the porous media, but due to the agglomeration of drops needed to block each pore closer to the ending of the flow the number of free drops is reduced, when created with similar parameters to others sizes, leading to fewer blocked pores in the final sections.

Differently, the flooding process performed with the higher flow rate demonstrated an inefficient aspect of the emulsion flooding as the initial residual oil is very low, the injected drops are unable to significantly increase pressure or create new paths via blockage. Still, the results indicated that larger drops are slightly more efficient in this scenario, as a droplet considerably larger than the channel and the pores are more likely to be able to resist the increased flow pressure and block the pores.

The experiments indicated considerable difference in the emulsion flooding due to the size of the injected drops in comparison to the size of the pores as well as with the capillary number of the injection process, demonstrating a clear difference for each scenario. This leads to the conclusion that for an emulsion flooding to be performed on a porous media under specific characteristics there is a particle size that better fits the situation leading to a maximum recovery.

Bibliography

- [1] E. S. P. B. V, F. Durst, R. Haas, and W. Interthal, "The nature of flows through porous media," vol. 22, pp. 169–189, 1987.
- [2] J. R. Philip, "Flow in porous media," 1970.
- [3] J. R. Fanchi, "Developments in Petroleum Science Volume 49," pp. 41–56.
- [4] O. Elmofty, "Surfactant enhanced oil recovery by wettability alteration in sandstone reservoirs," 2012.
- [5] L. Cao, "Superhydrophobic Surface: Design, Fabrication, and Applications," 2010.
- [6] C. Agbalaka, A. Y. Dandekar, and S. L. Patil, "The Effect of Wettability on Oil Recovery : A Review," 2008.
- [7] M. M. Honarpour, G. V Chilingarian, and S. J. Mazzullo, *Permeability and Relative Permeability of Carbonate Reservoirs*, vol. 30. .
- [8] S. M. Skjaeveland, L. M. Siqveland, A. Kjosavik, W. L. Hammervold, and G. A. Virnovsky, "Capillary Pressure Correlation for Mixed-Wet Reservoirs SPE 39497 Capillary Pressure Correlation for Mixed-Wet Reservoirs," no. February 2000, 2017.
- [9] V. P. Dimri, R. P. Srivastava, and N. Vedanti, "Reservoir Geophysics: Some Basic Concepts," *Handb. Geophys. Explor. Seism. Explor.*, vol. 41, pp. 89–118, 2012.
- [10] V. J. Niasar and S. M. Hassanizadeh, "Dynamics of two-phase flow in porous media : From Pore scale to Darcy scale Analysis of Fundamentals of Two-Phase Flow in Porous Media Using Dynamic Pore-Network Models : A Review," no. January 2016.
- [11] B. J. G. M, and C. B, "Secondary Recovery of Oil," *Futur. Supply Nature-Made Pet. Gas*, pp. 397–410, 1977.
- [12] G. P. Willhite, *Waterflooding*. 1986.
- [13] F. D. Martin, *Reservoir Engineering*. Gulf Publishing Company.
- [14] Forrest F. Craig Jr, "Reservoir Engineering Aspects of Waterflooding."
- [15] B. S. Engelke and M. S. Carvalho, "Determinação das Curvas de Permeabilidade Relativa no Escoamento de Emulsões e Óleo," 2012.
- [16] R. V. P. F, M. S. Carvalho, and V. Alvarado, "Oil recovery modeling of macro-emulsion flooding at low capillary number," *J. Pet. Sci. Eng.*, vol. 119, pp. 112–122, 2014.

- [17] M. Y. Khan, Z. A. A. Karim, F. Y. Hagos, A. R. A. Aziz, and I. M. Tan, "Current Trends in Water-in-Diesel Emulsion as a Fuel," vol. 2014, 2014.
- [18] M. K. Sharma and D. O. Shah, "Introduction to Macro- and Microemulsions," 1985.
- [19] W. C. Griffin, "Classification of surface-active by 'HLB,'" pp. 311–326, 1949.
- [20] S. F. Wong, J. S. Lim, and S. S. Dol, "Crude oil emulsion: A review on formation, classification and stability of water-in-oil emulsions," *J. Pet. Sci. Eng.*, vol. 135, pp. 498–504, 2015.
- [21] Krüss, "Critical Micelle Concentration." [Online]. Available: <https://www.kruss-scientific.com/services/education-theory/glossary/critical-micelle-concentration-cmc-and-surfactant-concentration/>.
- [22] W. D. Bancroft, "The Theory of Emulsification V.," vol. 3, no. 1904, pp. 501–519, 1913.
- [23] H. J. Butt, K. Graf, and M. Kappl, "Physics and Chemistry of Interfaces 3rd Edition."
- [24] D. E. G. Campos and M. S. Carvalho, "Formação de emulsões em uma junção de micro canais em T," 2011.
- [25] X. Liang, J. Wu, X. Yang, Z. Tu, and Y. Wang, "Investigation of oil-in-water emulsion stability with relevant interfacial characteristics simulated by dissipative particle dynamics," *Colloids Surfaces A*, vol. 546, no. December 2017, pp. 107–114, 2018.
- [26] P. Sciences, "Emulsion Stability and Testing," 2011.
- [27] I. Macuzic, M. Djapan, and M. Milosevic, "Influence of processing on cosmetic , pharmaceutical and food emulsions quality , stability and rheology," in *7th International Quality Conference*, 2013, no. January 2016.
- [28] T. Fu, Y. Ma, D. Funfschilling, C. Zhu, and H. Z. Li, "Squeezing-to-dripping transition for bubble formation in a microfluidic T-junction," *Chem. Eng. Sci.*, vol. 65, no. 12, pp. 3739–3748, 2010.
- [29] G. T. Vladislavljevi, R. Al Nuamani, and S. A. Nabavi, "Microfluidic Production of Multiple Emulsions Microfluidic Production of Multiple Emulsions," no. March, 2017.
- [30] C. D. McAuliffe, "Oil-in-Water Emulsions and Their Flow Properties in Porous Media."
- [31] D. P. Schmidt, H. Soo, and C. J. Radke, "Linear Oil Displacement by the Emulsion Entrapment Process," no. June, pp. 351–360, 1984.
- [32] J. Bryan, J. Wang, and A. Kantzas, "Measurement of emulsion flow in porous media : Improvements in heavy oil recovery," no. March 2009, 2017.
- [33] S. Cobos, M. S. Carvalho, and V. Alvarado, "Flow of oil – water emulsions through a constricted capillary," *Int. J. Multiph. Flow*, vol. 35, no. 6, pp. 507–515, 2009.
- [34] V. R. Guillen, M. S. Carvalho, and V. Alvarado, "Pore Scale and Macroscopic Displacement Mechanisms in Emulsion Flooding," pp. 197–206, 2012.

- [35] M. Moradi, M. Kazempour, J. T. French, and V. Alvarado, “Dynamic flow response of crude oil-in-water emulsion during flow through porous media,” *FUEL*, vol. 135, pp. 38–45, 2014.
- [36] A. Baldygin, D. S. Nobes, and S. K. Mitra, “Water-alternate-emulsion (WAE): A new technique for enhanced oil recovery,” *J. Pet. Sci. Eng.*, vol. 121, pp. 167–173, 2014.
- [37] M. L. R. de Farias, E. F. Campos, A. L. S. de Souza, and M. S. Carvalho, “Injection of Dilute Oil-in-Water Emulsion as an Enhanced Oil Recovery Method for Heavy Oil : 1D and 3D Flow Configurations,” *Transp. Porous Media*, vol. 113, no. 2, pp. 267–281, 2016.
- [38] A. Perazzo, G. Tomaiuolo, V. Preziosi, and S. Guido, “Emulsions in porous media : From single droplet behavior to applications for oil recovery,” *Adv. Colloid Interface Sci.*, vol. 256, pp. 305–325, 2018.
- [39] N. M. de Lima and M. S. Carvalho, “Análise do Deslocamento de Óleo por Soluções Poliméricas em Microescala,” 2015.
- [40] J. A. Avendaño, N. M. Lima, J. A. Quevedo, and M. S. Carvalho, “Effect of capillary-driven snap-off on fluid displacement in microfluidic porous media with different surface wettability,” in *The Society of Reology 89th Annual Meeting*.